

Laboratory of Materials (LoM)

**“Effect of homogenization time, temperature and cooling practice on the  
hardness and microstructure of 6xxx aluminum alloys”**

Diploma Thesis

Tousias Alexandros - Spyridon

Supervisor: G.N.Haidemenopoulos



Volos, Greece 2014



**ΠΑΝΕΠΙΣΤΗΜΙΟ ΘΕΣΣΑΛΙΑΣ**  
**ΒΙΒΛΙΟΘΗΚΗ & ΚΕΝΤΡΟ ΠΛΗΡΟΦΟΡΗΣΗΣ**  
**ΕΙΔΙΚΗ ΣΥΛΛΟΓΗ «ΓΚΡΙΖΑ ΒΙΒΛΙΟΓΡΑΦΙΑ»**

Αριθ. Εισ.: 12887/1  
Ημερ. Εισ.: 10-09-2014  
Δωρεά: Συγγραφέα  
Ταξιθετικός Κωδικός: ΠΤ – ΜΜ  
2014  
ΤΟΥ

## Abstract

The 6xxx series (AL-Mg-Si) aluminum alloys are widely used for extrusion applications. After DC-casting the billets follow a homogenization cycle, which consists of a soaking treatment followed by cooling to room temperature. The controlling factor for the selection of the homogenization parameters is the  $\beta$ -AlFeSi to  $\alpha$ -AlFeSi transformation as other transformations (e.g the Mg<sub>2</sub>Si dissolution) are much faster.

The effect of homogenization practice on 6xxx series aluminum alloys has been studied experimentally. Three cast billets with different compositions, corresponding to 6082, 6005 and 6063 alloys were considered. Homogenization treatments were performed at soak temperatures from 540 to 580°C and times of 30 minutes to 32 hours, while three different cooling rates were considered: water cooled, air-cooling (naturally in the air), forced air cooling by a fan. Brinell hardness measurements were conducted on the as-homogenized specimens and after natural aging for 5 days. The as-cast microstructure of the 6082 alloy was examined through optical microscopy and was compared to the microstructure of the homogenized samples. In addition, quantitative metallography was employed in order to measure the volume fractions of the Mg<sub>2</sub>Si and  $\alpha$ + $\beta$  AlFeSi phases in the as-cast state of the 6082 alloy and compared simulation predictions from Scheil solidification with Thermo-Calc.

It was found that in all three alloys, the samples soaked for 8 hours at all homogenization temperatures exhibited the lowest hardness after homogenization treatment but in contrast they had the higher age hardening potential. Regarding the effect of cooling rate and alloying elements, it was shown that increasing the cooling rate produced higher hardness while decreasing Mg and Si compositions produced lower hardness on the as homogenized samples.

The results can be used for the validation of modeling predictions regarding the phase transformations during homogenization and the selection of optimum homogenization parameters.

## **Acknowledgements**

The completion of this dissertation would not have been possible without the help of several people whom I would like to thank:

- I am grateful to my professor Prof. G.N. Haidemenopoulos for providing me this opportunity to work on this project and for his encouragement and guidance both personally and professionally. I owe to him many thanks for his direction and teaching during my studies.
- Could not disregard to thank Prof. Aravas Nikolaos and Prof. Kermanidis Alexis for their careful reading of my thesis.
- I would like to thank the staff of the laboratory of materials of the University of Thessaly but especially Panagiota Sarafoglou. During my dissertation I had a great support of Panagiota which encouraged me. She was very patient and helped me in many aspects of my thesis.
- I would also like to express my appreciation to my family and my friends. I am especially grateful to them all.

# Contents

Chapter 1 .....	- 6 -
Introduction .....	- 6 -
Problem definition .....	- 7 -
1.1 Aluminum alloys .....	- 7 -
1.1.1 Heat treatable aluminum alloys .....	- 8 -
1.1.2 Applications .....	- 10 -
1.2 Thermal history of an extrusion billet .....	- 11 -
1.3 Thesis Outline .....	- 14 -
Chapter 2 .....	- 15 -
Literature Review .....	- 15 -
2.1 The as-cast microstructure - Its effect on the extrudability .....	- 16 -
2.2 Major steps of homogenization treatment .....	- 19 -
2.3 Precipitation hardening (aging) – Hardening thermal treatment .....	- 21 -
Chapter 3 .....	- 24 -
Experimental Procedures .....	- 24 -
3.1 Methodology and materials .....	- 25 -
3.2 Sectioning .....	- 25 -
3.3 Metallography .....	- 27 -
3.4 Homogenization and quenching process .....	- 27 -
3.5 Hardness measurements .....	- 28 -
Chapter 4 .....	- 30 -
Results and Discussion .....	- 30 -
4.1 The as-cast microstructure .....	- 31 -
4.2 Metallographic observations – Optical microscopy .....	- 33 -
4.2.2 Validation of the volume fractions of intermetallic phases .....	- 35 -
4.2.3 Time evolution of the microstructure of 6082 during homogenization .....	- 38 -
4.3 Hardness measurements - Immediately after homogenization and after natural ageing ..	- 42 -
Chapter 5 .....	- 58 -
Conclusions .....	- 58 -
References .....	- 62 -
Appendix .....	- 65 -

1. Spheroidization mechanism of the $\beta$ -AlFeSi to $\alpha$ -Al(FeMn)Si transformation .....	- 65 -
2. Specimen regularization tables 2.1 6082 aluminum alloy .....	- 67 -
2.2 6005 aluminum alloy .....	- 68 -
2.3 6063 aluminum alloy .....	- 69 -

# Chapter 1

## Introduction

*In this chapter, the special properties and its applications of aluminum 6xxx series alloys are provided. The stages of the manufacturing process of these alloys, namely, solidification, homogenization, quenching, ageing, extrusion are also presented.*

## Problem definition

Extrusions are a particularly important forming process on the manufacturing industry and 6xxx series are often the optimal choice for extrusion applications due to the ease and the economical way they extrude. The homogenized billets extrude easier and faster and give higher tensile properties than as-cast billets. However there are limits to how much a homogenization treatment can improve the performance of the billet. Several features of the billet must be taken into account before homogenization, such as the billet composition which is crucial for the as-cast microstructure, the grain structure, the surface finish and others. When properly homogenized an aluminum billet, will give optimum extrusion parameters.

An industrial homogenization treatment typically consists of a soaking treatment which is followed by a cooling. During this homogenization treatment several processes take place such as the transformation of the plate-like  $\beta$ -AlFeSi intermetallics to the more rounded  $\alpha$ -AlFeSi particles. The  $Mg_2Si$  phase dissolution takes place during homogenization and is important as it gives the age hardening potential for the extruded product. However, the dissolution of the  $Mg_2Si$  phase is fast compared with the  $\beta$  to  $\alpha$  transformation. So, the homogenization time is mainly controlled by this transformation. The  $\beta$ -AlFeSi phase induces local cracking and surface defects in the extruded material and as a result the  $\beta$  to  $\alpha$  transformation is important as it improves the extrudability of the material. The motivation behind controlled cooling after homogenization is to reprecipitate  $Mg_2Si$  in a form and size easily redissolvable during subsequent processing.

The present work was undertaken to investigate the effect of the homogenization parameters, time, temperature and cooling rate on the as-homogenized hardness and on microstructure of three aluminum alloys, 6082, 6005 and 6063.

### 1.1 Aluminum alloys

Aluminum is of the most abundant metallic elements on earth. Its low density ( $2.70 \text{ g/cm}^3$ ), approximately one-third as much as steel ( $7.83 \text{ g/cm}^3$ ), copper ( $8.93 \text{ g/cm}^3$ ), or brass ( $8.53 \text{ g/cm}^3$ ) makes it applicable on engineering structures and products requiring high strength to weight ratio. It can display excellent corrosion resistance in most environments, including atmosphere, water (including salt water), petrochemicals, and many chemical systems. In addition, aluminum typically displays excellent electrical and thermal conductivity. Pure aluminum is only used in a limited way commercially, and is typically alloyed with other elements to obtain strength or other desired properties. The most common elements used are copper (Cu), manganese (Mn), silicon (Si), magnesium (Mg), zinc (Zn).

The International Alloy Designation System (IADS) has enacted a four-digit numerical designation system that is used to identify wrought aluminum and aluminum alloys. The first digit of this system indicates the group and its main components as shown on the table below:



Aluminum, $\geq 99\%$	1xxx
Aluminum alloys grouped by major alloying element(s):	2xxx
Copper	
Manganese	3xxx
Silicon	4xxx
Magnesium	5xxx
Magnesium and silicon	6xxx
Zinc	7xxx
Other elements	8xxx
Unused series	9xxx

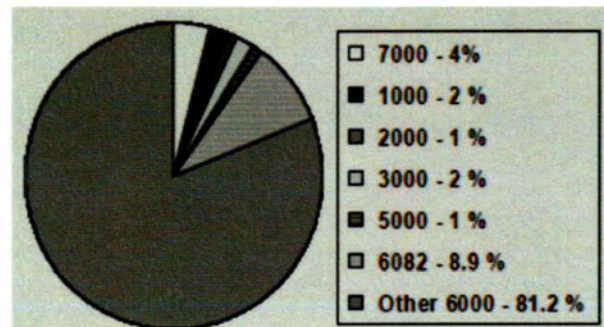
### 1.1.1 Heat treatable aluminum alloys

Heat treatable aluminum alloys are those that can be hardened (strengthened) by a controlled cycle of heating and cooling. Some alloys, usually in the 2xxx, 6xxx and 7xxx series, are solution heat treatable – they can be strengthened by heat treating and then quenching, or rapid cooling. The increase of strength induced heat treatment can be dramatic.

The aluminum alloys which are amenable to heat treatment are characterized from a symbol T followed by a number. The symbol enacted by the Temper Designation System and “means” solution heat treated, while the number follows represents a specific sequence of basic treatments. The tempers used are listed above:

- **T1**, Cooled from an elevated-temperature shaping process and naturally aged to substantially stable condition.
- **T2**, Cooled from an elevated-temperature shaping process, cold-worked, and naturally aged to a substantially stable condition.
- **T3**, Solution heat treated, cold worked, and naturally aged to a substantially stable condition.
- **T4**, Solution heat treated and naturally aged to a substantially stable condition.
- **T5**, Cooled from an elevated-temperature shaping process and artificially aged.
- **T6**, Solution heat treated and artificially aged.
- **T7**, Solution heat treated and over-aged or stabilized.
- **T8**, Solution heat treated, cold worked, and artificially aged.
- **T9**, Solution heat treated, artificially aged, and cold worked.
- **T10**, Cooled from an elevated-temperature shaping process, cold worked, and artificially aged.

**Aluminum alloys 6xxx series** contain as major alloying elements magnesium and silicon which produce the compound magnesium-silicon ( $Mg_2Si$ ). The formation of this compound provides the 6xxx series their heat-treatability. Extrusions are a particularly important forming process on the manufacturing industry and 6xxx series are often the optimal choice for extrusion applications due to the ease and the economical way they extrude (**Fig.1.1**). **Figure 1.1** shows the unambiguous domination of the 6xxx alloy system on the extrusion industry. Although these alloys are not that strong as those of 7xxx and 2xxx series, they can be age hardened due to the presence of  $Mg_2Si$  phase which offers to the alloy age hardening potential. There are various additional advantages in the use of these alloys such as their good ductility and formability and their corrosion resistance even in marine environments. Moreover they are easy to weld and therefore are found widely throughout the welding fabrication industry. On the other hand these alloys have their own disadvantages which include the fact that they are more expensive than steels, its difficulty to separate from other materials despite their recyclability and the effect of natural ageing on their subsequent heat treatments.

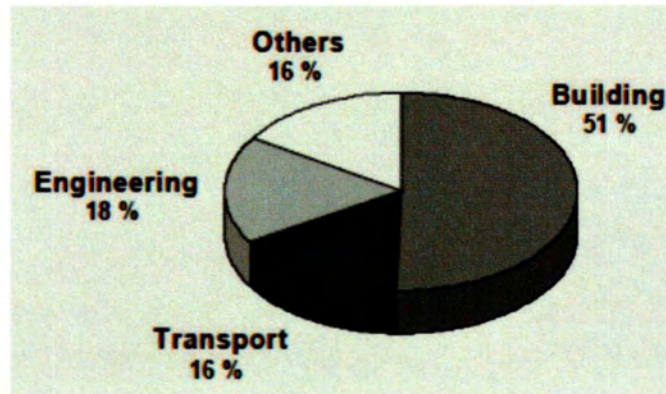


**Fig.1.1** Aluminum alloys used for extrusion purposes, Europe, 2000 [1]

Among the 6000 series, the 6060 alloy offers medium strength and is easy to extrude even for complicated cross-sections. The 6063 alloy has slightly higher strength than 6060, but is marginally more difficult to extrude. It provides high quality surface finish after extrusion and it is the most widely used alloy. Both 6063 and 6060 are well suited for anodizing, both for decorative and protective reasons. Aluminum alloy 6082 is a medium strength alloy with high corrosion resistance. It has the highest strength of the 6xxx series alloys. It is widely used for structural applications. The addition of a large amount of manganese controls the grain structure which in turn results in a stronger alloy. Alloy 6082 offers good weldability, machinability, corrosion resistance and formability. The extruded surface finish is not as smooth as other similar strength alloys in the 6000 series. 6005 aluminum alloy is also a medium strength alloy, but its strength is higher than 6063's alloy, and contains high amounts of silicon. These alloys are used in designs that require moderate strength and can also be welded and brazed satisfactorily. In general the 6005, 6063, 6082 should not be used in structures at temperatures above  $100^{\circ}C$ . The tensile strength decreases as the temperature increases while elongation on fracturing usually increases. In the present work the focus has been on 6005, 6063 and 6082 alloys.

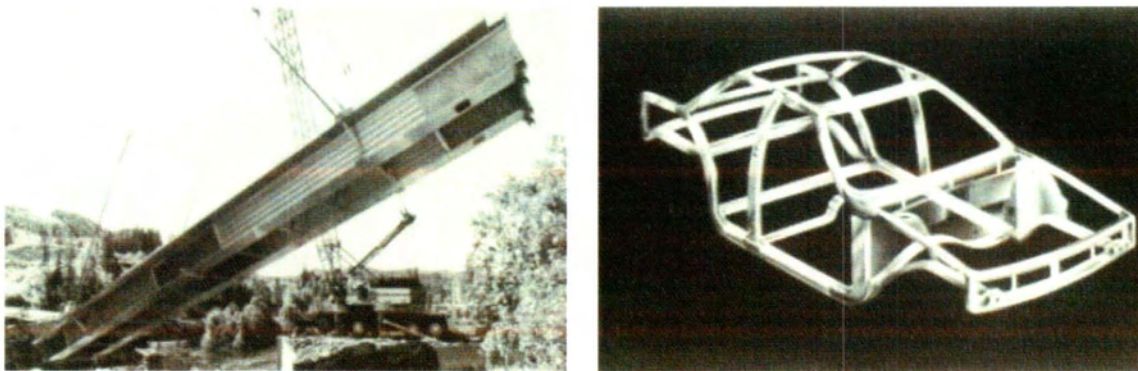
### 1.1.2 Applications

The 6xxx-group alloys have a wide range of applications, especially in the building, aircraft and automotive industry due to their excellent strength, weight and corrosion properties. Then main market for extruded products is the building sector (**Fig.1.2**) while the transportation sector is very challenging for further investigation and developments on these alloys.



**Fig.1.2** Markets for extruded products, Europe, 2001 [1]

Alloy 6063 is perhaps the most widely used because of its extrudability. That property makes them the first choice for architectural and structural members where strength or stiffness is important. A good example of its structural use was the all-aluminum bridge in Foresmo, Norway (**Fig.1.3a**). This alloy is in addition, the first choice for the Audi automotive space frames members (**Fig.1.3b**). 6111 aluminum alloy is extensively used in the automotive industry to produce body panels. Aluminum alloys that are used for boat building and shipbuilding, and other marine alloys and salt-water sensitive shore applications are 6063 and 6061. 6082 and 6005 are also used in marine constructions and off shore applications. Simultaneously 6063 and 6061 alloys are commonly used in aircraft and other aerospace structures. Representative important applications of the 6xxx alloy series are shown in the figures following (**Fig 1.4-6**).



**Fig.1.3** Extruded 6xxx aluminum alloys a) the Foresmo bridge in Norway made by 6063 b) the entire body frame of the Audi A8 [2]



Fig. 1.4 The roof structures for arenas and gymnasiums are usually 6063 or 6061 extruded tube, covered with 5xxx alloy sheet. [2]

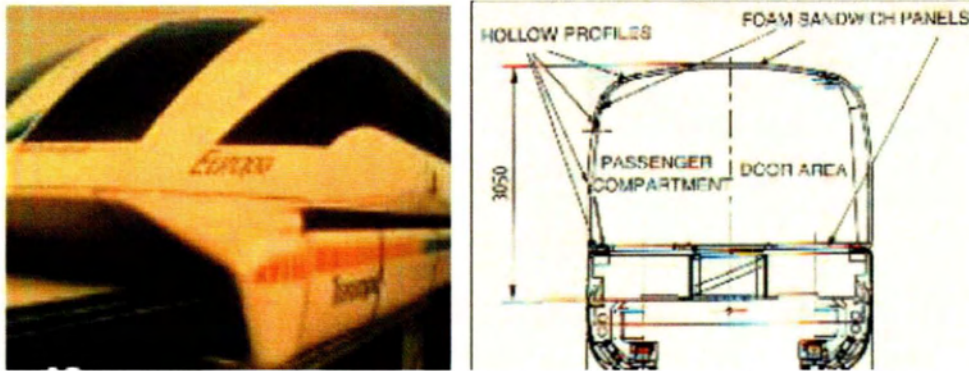


Fig. 1.5 The new Mag-Lev trains in development in Europe and Japan employ bodies with 6061 and 6063 structural members. [2]

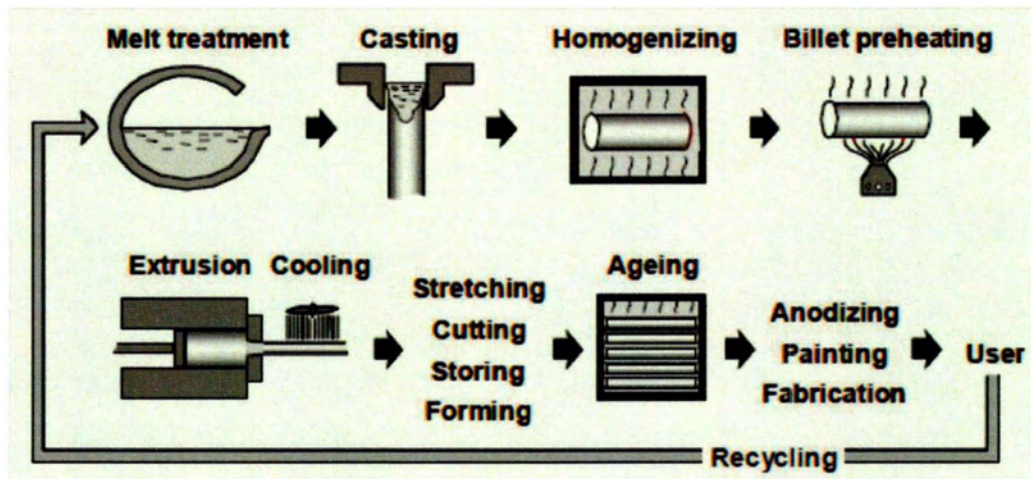


Fig. 1.6 The power of extruded Al-Mg-Si alloys is the "put the metal where you need it" flexibility that these alloys and the extrusion process provide.[2]

## 1.2 Thermal history of an extrusion billet

The most heat treatable aluminum alloys are heat treated to obtain the desired combination of properties, such as strength, ductility and provision of better surface finish. The main

purpose among the heat treatment of 6xxx alloys is the improvement on their extrudability. **Figure 1.7** represents a sketch of the different process steps that are carried out in the production of aluminum extrusion profiles. Melt treatment and alloying, DC casting and usually homogenization of the ingots are done in the cast house. Afterwards the ingots are transferred to the extrusion plants where they are preheated, extruded, cooled, formed and in an optional final step the extrusion profiles are artificially age-hardened.

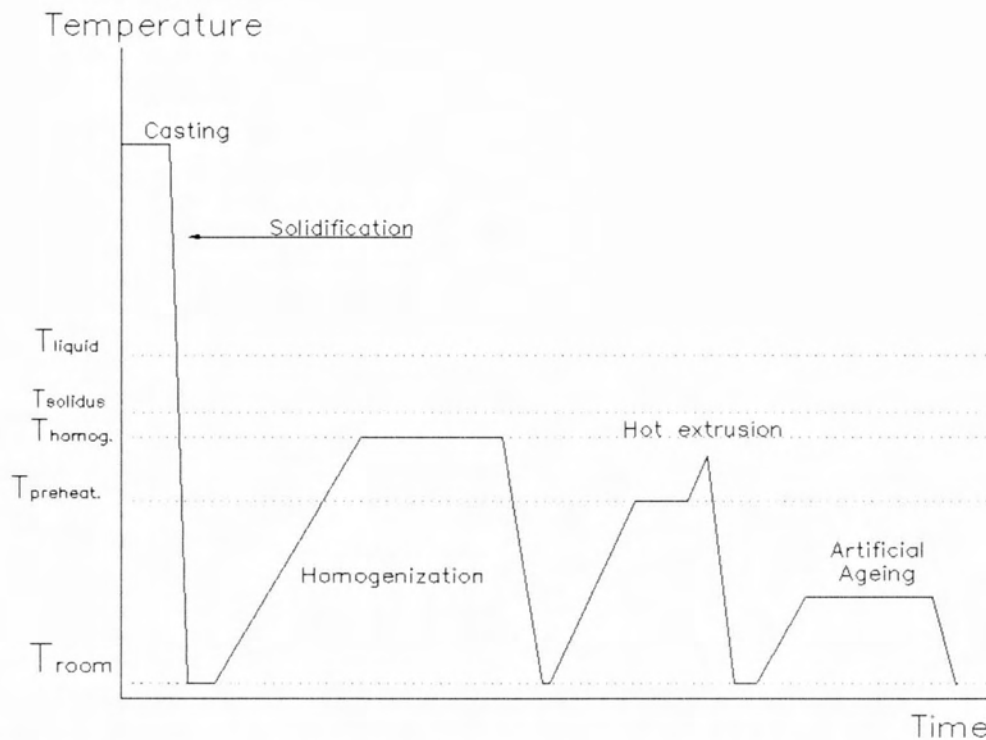


**Fig.1.7** Sketch of the different process steps related to the production of extrusions [3]

Consider the examples of AlMgSi aluminum alloys given on chapter 1.1.1. The most important factor that these products have in common is that they are extruded. During hot extrusion of aluminum alloys an aluminum billet is pushed through a die by a ram at elevated temperatures, as depicted in **Figures 1.7-8**. In this way considerable lengths of material can be produced at high production speed, which have a good surface finish and a well-defined cross section within strict geometric tolerances. A need for higher production speeds, better mechanical properties, more complicated cross-sections and a better surface quality of the extrudate presented in the recent years. These demands often require better process control, die manufacturing technology and billet quality. The demands on the process control depend largely on the quality of the casting process of the extrusion billet, but in particular on the alloy composition.

The microstructure of a common AlMgSi extrusion alloy directly after casting is not suitable for extrusion. The inhomogeneous distribution of alloying elements severely limits the maximum extrusion speed below which the surface finish still meets the requirements (smooth surface, no cracks etc.) Furthermore, it causes poor mechanical properties of the extrudate, because of the low content of dissolved alloying elements available directly after extrusion. In principle there are two methods to prevent the presence of these inhomogeneities in the alloy directly before extrusion: 1) improving the casting method in order to obtain a more homogeneous as-cast alloy, and 2) homogenizing the as-cast billet via an additional high temperature heat treatment. The homogenization of the DC castings is very important as it gives significant microstructure changes, leading to an improvement on the extrudability of the material and improved properties of the final product. It is consisted of three stages: heating, soaking at the soak temperature for several hours and then cooling to room

temperature. On **Figure 1.8** it is shown the temperature and time-course of the production process mentioned above which includes typical homogenization times and temperatures.



**Fig.1.8** Schematic temperature path of the aluminum heating process during the production of extrusion profiles. Homogenization and extrusion processes are displayed.

After the billet is cast and solidified, the inhomogeneities are reduced by homogenizing at a temperature which is high enough to enable dissolution and diffusion of secondary phases: precipitates, segregates and other intermetallic compounds. Most of the secondary phases consist of impurity elements or deliberately added alloying elements and are formed during solidification and subsequent cooling to room temperature. After homogenization the billet is cooled to room temperature as fast as possible. The homogenized billet can now be extruded to an extrusion plant. At the extrusion plant the homogenized billet is put in pre-heating furnace and preheated to the deformation temperature. Subsequently, the preheated billet is inserted into the billet container and extruded. During extrusion the temperature rises further due to internal friction caused by the deformation process. The extrudate is cooled to room temperature and is subsequently artificially aged at a temperature of approximately 185°C to improve the mechanical properties.

The thermal history during the extrusion process involves homogenization, pre-heating before extrusion, an optional solutionizing treatment directly after extrusion, and artificial ageing. These heat treatments largely affect the alloy extrudability.

At the current thesis emphasis will be given on the homogenization process, namely the soaking and the cooling processes.

### **1.3 Thesis Outline**

This thesis emphasizes on the effect homogenization thermal treatment on the hardness and microstructure of the 6082, 6005 and 6063 aluminum alloys.

In chapter 2 a brief reference on the literature about the homogenization process is presented. In chapter 3 the methodology followed during the experimental procedure is described in detail, while in chapter 4 the results obtained from the experiment are given in tables and charts. Finally, in chapter 5 the main conclusions of this work are summarized.

## **Chapter 2**

### **Literature Review**

*In this chapter, the results of previous studies on the effect of homogenization temperature and time and on the effect of cooling practice on the 6xxx series alloys are reviewed. An overview on the as-cast microstructure and on the microstructure evolution at each stage (soaking, cooling) is given. A brief reference on the aging is also given.*



## 2.1 The as-cast microstructure - Its effect on the extrudability

The microstructure of an as-cast aluminum alloy after solidification consists of a collection of micro-structural aspects, which are listed below:

- Grain size: a grain consists of crystallite of the primary aluminum phase, the aluminum matrix, and is bound by other grains with a different orientation. Typical grain sizes in as-cast commercial AlMgSi alloys are of the order of 100-500 $\mu$ m. [3,4]
- Dendritic Arm Spacing (DAS) after casting: a grain in an as-cast alloy is dendritic, and either equiaxed or columnar in nature. The dendritic structure is often characterized by the spacing of the smallest dendrites, which represents a characteristic diffusion distance, and is typically on the order of 20-50 $\mu$ m in a commercial AlMgSi alloy. [3,4]
- Relatively stable dispersoids and intermetallic phases formed during casting, which may change their crystal structure at homogenization thermal treatment. (Tables 2.1-2) They remain relatively stable after homogenization. In commercial AlMgSi alloys these phases consist mainly of Al, Fe, Mn and Si.

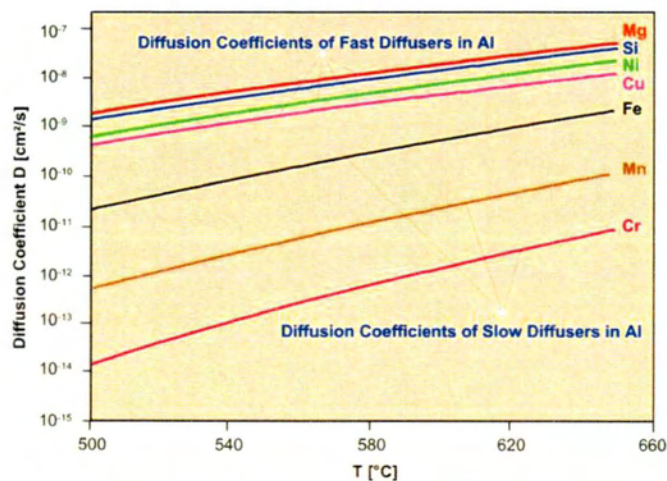
Table 2.1 Solidification reactions [3]

Reaction	Temperature (°C)
$L \rightarrow \alpha - Al$	650
$L \rightarrow Al + Mg_2Si$	587
$L \rightarrow Al + Si + Mg_2Si$	555
$L \rightarrow Al_{13}Fe_4 + \alpha - Al$	655
$L + Al_{13}Fe_4 \rightarrow \alpha - AlFeSi + \alpha - Al$	638
$L \rightarrow \alpha - AlFeSi + \alpha - Al$	580-610
$L + \alpha - AlFeSi \rightarrow \beta - AlFeSi + \alpha - Al$	612
$L \rightarrow \beta - AlFeSi + \alpha - Al$	611
$L \rightarrow \beta - AlFeSi + \alpha - Al + Si$	575
$L \rightarrow \beta - AlFeSi + Mg_2Si + \alpha - Al$	585
$L + \alpha - AlFeSi \rightarrow \alpha - Al + \beta - AlFeSi + Mg_2Si$	576
$L \rightarrow \alpha - Al(FeMn)Si + Mg_2Si + \alpha - Al + Si$	550

**Table 2.2** The structural variance of the prevalent intermetallic phases in 6xxx series [3]

Notation	Stoichiometry	Bravais lattice	Lattice parameters	Density ( $\delta$ ) kg/m <sup>3</sup>
$\beta$	Al <sub>4.5</sub> FeSi Al <sub>3</sub> FeSi	Moniclinic	a = 6.12A b = 6.12A c = 41.5A $\beta = 91^\circ$	3300 - 3350
$\alpha_h(\alpha)$	Al <sub>8</sub> Fe <sub>2</sub> Si	Hexagonal	a = b 12.3A c = 26.2A	3580
$\alpha_c$	(Fe containing) Al <sub>12</sub> Fe <sub>3</sub> Si Al <sub>12-15</sub> Fe <sub>3</sub> Si <sub>1-2</sub>	Cubic	a = 12.56A	3640
	(Fe + Mn containing) Al <sub>12</sub> (FeMn) <sub>3</sub> Si Al <sub>15</sub> (FeMn) <sub>3</sub> Si <sub>2</sub>	Cubic	a = 12.56 – 12.68A	3640 – 3630
	(Mn containing) Al <sub>12</sub> Mn <sub>3</sub> Si Al <sub>15</sub> Mn <sub>3</sub> Si <sub>2</sub> Al <sub>9</sub> Mn <sub>2</sub> Si	Cubic	a = 12.68A	3630

- Inclusions: stable impurity particles, which have somehow contaminated the alloy during casting.
- Macro and micro segregation: consisting of alloying elements segregated by solidifying dendrites during the solidification process. They may contain the intermetallic phases mentioned above and are relatively large. Their spatial distribution is determined by the dendritic structure.
- Precipitates: consisting of relatively fast diffusing elements, typically the primary alloying elements. In AlMgSi alloys these are Mg, Si as seen on **Fig. 2.1**, which create the Mg<sub>2</sub>Si particle.



**Fig2.1** Diffusion coefficients of fast and slow diffusers in aluminum. Alloys containing slow diffusers need longer heating times compared to those containing fast diffusers. For a given temperature, diffusion coefficients of fast and slow diffusers are by many orders of magnitude. [7]

- Solute alloying elements: mainly the primary alloying elements which are still present in solid solution in the aluminum matrix after cooling down from the casting process.

	Element	Max. Solubility (wt.%)
<b>High Solubility</b>	<b>Zn</b>	<b>70</b>
	<b>Mg</b>	<b>17.4</b>
	<b>Cu</b>	<b>5.65</b>
	<b>Mn</b>	<b>1.8</b>
	<b>Si</b>	<b>1.65</b>
<b>Low Solubility</b>	<b>Ti</b>	<b>1.3</b>
	<b>Cr</b>	<b>0.77</b>
	<b>Zr</b>	<b>0.28</b>
	<b>Fe</b>	<b>0.05</b>

Fig 2.2 Alloying elements solubilities in Al [7]

In commercial AlMgSi alloys all these aspects may be present.

Extrusion is a process characterized by large and transient plastic deformations, with high dislocation densities. [8] The effect of the micro-structural aspects on the extrudability can often be understood in terms of their restricting effect on the movement of the dislocations and their effect on the surface quality of the alloy. Most of the aspects listed above influence the extrudability, which means:

1. The mechanical properties are largely dependent on alloying elements present in solid solution, such as Mg, Si. These elements increase the strength through solid solution or precipitation hardening resulting on lower machinability. They act as obstacles on the dislocation movement and, therefore, increase the high temperature strength of the alloy resulting in a high extrusion pressure. [1, 8-9]
2. The inclusions, dispersoids and intermetallics enhance the formation of the precipitates during some of the heat treatments, and, if they are present in high densities of small particles, increase the extrusion pressure through their interaction with dislocations in motion.
3. Segregation can result in the formation of eutectic constitutive (low melting point) particles in the grain boundary regions or inside the grains. [10-12] These may be intermetallic phases, Mg<sub>2</sub>Si or Si phases. The presence of the particles which may cause incipient melting can deteriorate the hot workability of the aluminum alloys.
4. In addition, the formation of some hard particles with sharp edges e.g. Fe in combination with some alloying elements such as Mn and Si decrease the extrudability. The transformation of the  $\beta$ -AlFe(Mn)Si to  $\alpha$ -AlFe(Mn)Si particles is crucial for the extrudability of the alloy. The sharp tips of the  $\beta$  particles initiate micro-cracks during the deformation, and therefore start cracking the aluminum surface. In addition, the  $\beta$  plates, with a high coverage of the dendrites, block dislocations by interconnected network, making it difficult to deform the

material, whereas the more rounded small  $\alpha$  particles allow the dislocation to move around, making it easier for the material to change its shape. [10,12, 14]

5. The improvement on the extrudability is also associated with the Mg<sub>2</sub>Si phase distribution and its size. Large Mg<sub>2</sub>Si precipitates do not dissolve during extrusion and as a result the required extrusion pressure increases.

## 2.2 Major steps of homogenization treatment

The mechanical properties of aluminum alloys are largely dependent on alloying elements present in solid solution. These elements increase strength mainly through solid solution strengthening or precipitation. [11] As it was mentioned above, during casting of aluminum alloys, a large fraction of alloying elements segregate to the liquid and form constitutive particles in the grain boundary regions or inside the grains. [10] These particles decrease the hot workability and therefore limit the range of process parameters applicable during subsequent extrusion. [1, 15] It is well known that coarse residual particles deteriorate the extrudability of these alloys, especially when they are located in the grain boundary regions. [16-17] Therefore, it is necessary to dissolve these particles in the structure in order to obtain high mechanical properties and extrudability. In general, the aims of homogenization treatment may include the following: [11]

- Removing the inhomogeneous distribution of alloying elements due to microsegregation occurring during direct-chill (DC) casting.
- Dissolving the detrimental particles with low melting points which may result in tearing during hot extrusion.
- Dissolving the hard particles such as intermetallic phases or rounding the ones with sharp edges which can lead to poor ductility.
- Promoting the formation of nano-sized dispersoids for controlling the grain structure during and after hot deformation.

Homogenization comprises three major steps, heating billet with a particular rate, holding a constant temperature for a certain time, and cooling with a proper cooling rate. After direct chill (DC) solidification, the solid solution is supersaturated and the supersaturation increases from the center through the edges of the dendritic branches because of microsegregation. The first transformation that takes place is nucleation and growth of the particle phases Fe, Mn and Mg<sub>2</sub>Si which redissolve as the temperature rises.

While holding the billet at an elevated temperature for a specific time, diffusion is enhanced, and any concentration gradients within the alloy are diminished. The controlling factor in the homogenization of an alloy is thus the diffusivity of the respective alloying elements present at the homogenization temperature. The higher the homogenization

temperature is, the faster homogeneity can be obtained and, thus, the more efficient this practice becomes in terms of industrial throughput. The homogenization temperature, however, should not exceed the lowest melting point temperature in the particular alloy, which results in localized melting. This melting could cause structural damage of a type that cannot be repaired subsequently. This damage consists of excessive void formation, segregation, blistering and cracking.[15] The melting point of the material cannot be predicted from the phase diagram because the microstructure is on t the equilibrium one. As a result of microsegregation high concentration of alloying elements regions are melted on temperatures lower than the liquidus line. On **Fig. 2.3** the eutectic melting temperatures are presented. Another transformation that takes place is the particles coarsening, the rounding of the non-dissolvable ones and the transformation of the  $\beta$ -AlFeSi to the  $\alpha$ -AlFeSi.[**Appendix 1**] The  $\beta$ -to- $\alpha$  phase transformation considerably improves the extrusion process of the aluminum since the transformed  $\alpha$ -particles in the homogenized material improve the ductility of the material and the surface quality of the extruded material. [1, 12, 14-15] Additional microstructural changes, such as the dissolution of Mg<sub>2</sub>Si or Si particles, also occur during homogenization. However, since the Mg<sub>2</sub>Si or Si particles dissolve rather fast, it is the  $\beta$ -to- $\alpha$  transformation kinetics which determines the minimum homogenization time that is needed to get the material in a suitable state for extrusion.

**Table 2.3** Eutectic melting temperatures in Al-Mg-Si alloys [12]

<b>Melting Temperature</b>	<b>Reaction</b>
~575°C	$\text{Al} + \beta - \text{AlFeSi} + \text{Si} \rightarrow \text{Liquid}$
~576°C	$\text{Al} + \beta - \text{AlFeSi} + \text{Mg}_2\text{Si} \rightarrow \text{Liquid} + \alpha_h - \text{AlFeSi}$
~577°C	$\text{Al} + \text{Si} \rightarrow \text{Liquid}$
~587°C	$\text{Al} + \text{Mg}_2\text{Si} \rightarrow \text{Liquid}$
~612°C	$\text{Al} + \beta - \text{AlFeSi} \rightarrow \text{Liquid} + \alpha_h - \text{Al(FeMn)Si}$
~630°C	$\text{Al} + \alpha_h - \text{AlFeSi} \rightarrow \text{Liquid} + \text{Al}_3\text{Fe}$

Cooling of the billet after homogenization is very important to get the good microstructure to improve productivity as well as the final mechanical properties of the extrusion. A fully solutionized billet, as obtained at the end of soaking, is difficult to extrude. So, in contrast to soaking which is undertaken to achieve homogenization, the motivation behind controlled cooling is heterogenization.[4-5] During cooling from room temperature it takes place precipitation of Mg<sub>2</sub>Si, Fe, Mn and Cr particles. The size and the density of these particles is crucial because it balks the recrystallization of the material [15], which is beneficial for the final mechanical properties. Respectively, the size and the density of Mg<sub>2</sub>Si must be such that at the beginning of the extrusion process the alloying elements concentration in the matrix to be the minimum in order to decrease the strength of the material and increase the formability. [19, 21-22] In addition, the Mg<sub>2</sub>Si particle size should be relatively small, so that to dissolve during extrusion, and decreasing the dissolution time. [3-4, 15] The amount of Mg and Si in solid solution, and hence the amount of Mg<sub>2</sub>Si precipitated, are highly affected by the cooling from the homogenization temperature. Slow cooling tends to produce coarse Mg<sub>2</sub>Si particles

while rapid cooling trap the Mg and Si in solution with little or no Mg<sub>2</sub>Si precipitation.[1,22-24] Decreasing the cooling rate found to increase the Mg<sub>2</sub>Si precipitation and decrease the amount of Mg in solid solution. Mn additions up to 0.027% have no effect on Mg<sub>2</sub>Si precipitation. [22-25]

From literature, it is obvious the increasing interest to research on the field of the extrusion heat treatments of aluminum alloys, through last decades. Common characteristic of the works already performed is the correlation among the material microstructure and the extrudability, aiming to the maximization of the extrusion velocity. Several works have done on the Mg<sub>2</sub>Si particles dispersion after cooling from the homogenization temperature. Zajac et al. [19] and Nowotnik et al. [25] investigated the effect of the cooling rate on the final mechanical properties of the 6005, 6082 and 6063 aluminum alloys. Usta et al. [26] and van de Langkruis [20] studied the dissolution-coarsening kinetics of the Mg<sub>2</sub>Si particles during reheating. Reiso et al. [1] correlated the cooling rate to the maximum extrusion velocity for various chemical compositions of AlMgSi alloys. Birol et al. [4, 5] studied the effect of the homogenization temperature and time and the effect of cooling rate on the microstructure of 6063 and 6082 alloys through metallographic techniques. Kuijpers et al. [14] simulated the dependence of the  $\beta$ -AlFeSi to  $\alpha$ -Al(FeMn)Si transformation kinetics on the alloying elements and found a significant effect of the Mn concentration as it increases the transformation rate by increasing its concentration. Haidemenopoulos et al. [28] modeled the transformation of iron intermetallics during homogenization of 6xxx alloys. Finally, P.I.Sarafoglou and Haidemenopoulos [29] investigated the effects of alloying elements on intermetallic phase formation in the as cast microstructure via computational thermodynamics and found that additions of Mn lead to reduction of both the  $\beta$ -AlFeSi and Mg<sub>2</sub>Si phases in the as cast microstructure.

In this thesis an attempt to approximate the effect of homogenization time and temperature and the effect of cooling rate on the mechanical properties of 6082, 6005 and 6063 alloys was done. In addition, the effect of the same parameters on the microstructure of 6082 aluminum alloy was studied.

### **2.3 Precipitation hardening (aging) – Hardening thermal treatment**

The main characteristic of the heat treated aluminum alloys is that their final mechanical properties are owed on the precipitation of second phase particles. The basic alloying elements are Mg, Si, Cu, whose concentration exceed the maximum solid solubility, form particle dispersion during their heating, which finally contributes on the final strength of the material. [3]

The precipitation-hardening process involves three basic steps: Solution Treatment, Quenching and Aging. [29] These consist of heating the alloy to a temperature at which the soluble constituents will form a homogeneous mass by solid diffusion, holding the mass at that temperature until diffusion takes place, then quenching the alloy rapidly to retain the

homogeneous condition. In the quenched condition, heat-treated alloys are supersaturated solid solutions that are comparatively soft and workable, and unstable, depending on composition. At room temperature, the alloying constituents of some alloys tend to precipitate from the solution spontaneously, causing the metal to harden in about four days. This is called **natural aging**. Natural ageing may have a ‘negative’ effect on artificial aging. [30]

**Solution Treatment or Solutionizing**, is the first step in the precipitation-hardening process where the alloy is heated above the solvus temperature and soaked there until a homogeneous solid solution ( $\alpha$ ) is produced. The  $\theta$  precipitates are dissolved in this step and any segregation present in the original alloy is reduced.

**Quenching** is the sudden chilling of the metal in oil or water. The structure and the distribution of the alloying constituents that existed at the temperate just prior to cooling are “frozen”, into the metal by quenching. The properties of the alloy are governed by the composition and characteristics of the alloy, the thickness of cross section, and the rate at which the metal is cooled. It is the second step where the solid  $\alpha$  is rapidly cooled forming a supersaturated solid solution of which contains excess copper and is not an equilibrium structure. The atoms do not have time to diffuse to potential nucleation sites and thus  $\theta$  precipitates do not form.

**Aging** is the third step where the supersaturated is heated below the solvus temperature to produce a finely dispersed precipitate. Atoms diffuse only short distances at this aging temperature. Because the supersaturated  $\alpha$  is not stable, the extra copper atoms diffuse to numerous nucleation sites and precipitates grow. The formation of a finely dispersed precipitate in the alloy is the objective of the precipitation-hardening process. The fine precipitates in the alloy impede dislocation movement by forcing the dislocations to either cut through the precipitated particles or go around them. By restricting dislocation movement during deformation, the alloy is strengthened.

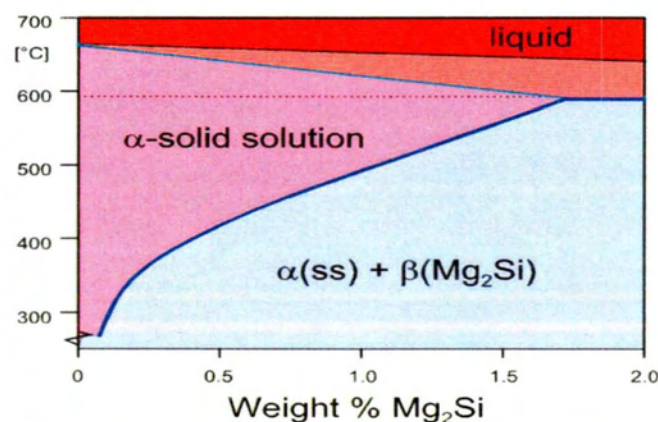


Fig 2.3 Equilibrium phase diagram of the Al-Mg<sub>2</sub>Si system [7]

The precipitation sequence of the particles is a complex process which contains various stages. In **Figure 2.4** it is shown the sequence of phases found during age hardening of Al-

Mg-Si alloys. It is compiled from various sources in the literature. [31-33] Supersaturated solid solution (SSSS) decomposes as Mg and Si atoms are attracted first to themselves (cluster) then to each other (co-cluster) to form precipitates GP(I), sometimes also called initial- $\beta''$ . GP(I) zones either further evolve directly to a phase  $\beta''$  and then to a number of other metastable phases labelled  $\beta'$ ,  $B'$ ,  $U1$ ,  $U2$  (another one,  $U3$ , has been postulated theoretically), or first form an intermediate phase called pre- $\beta''$ . The sequence depends on the Mg and Si content and the temperatures applied. The final equilibrium phase  $\beta$  is reached for higher temperatures only.[31]

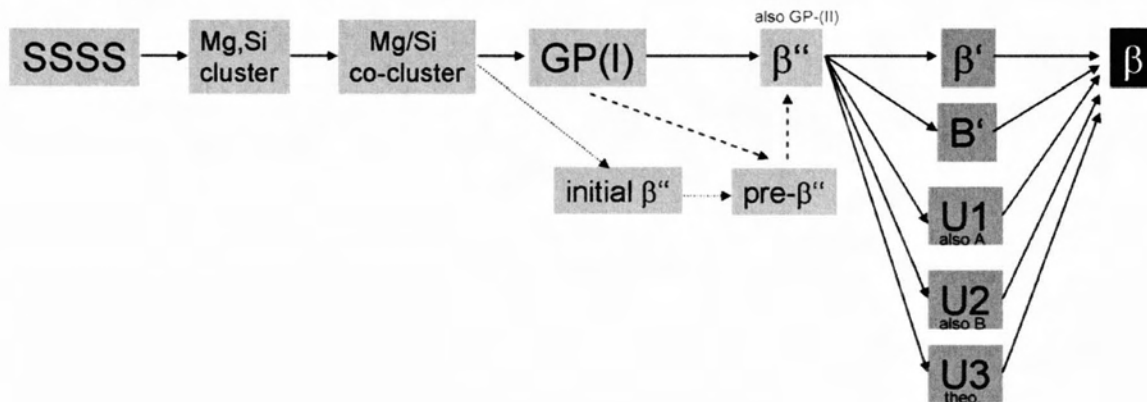


Fig 2.6 Sequence of phases found during age hardening of Al-Mg-Si alloys [30]

The precipitation sequence in Al-Mg-Si alloys has been investigated by many researchers and includes the stages listed in **Figure 2.6**. Such sequences are frequently given in publications, but one should remember that this is not a particular sequence valid for any temperature. Some of the phases might not occur at all at too low a temperature or may evolve into others almost instantaneously at too high a temperature and there may be ranges of co-existence of more than one phase. The exact precipitation sequence depends on the alloy composition (excess in Mg or Si) and the possible presence of additional elements (Cu, Mn, Fe). The phase in which the alloy owes its strength is the  $\beta''$  [36,37] while the  $\beta'$  phase does not contribute notably on the alloy strength. [34,35]

In this thesis just the effect of natural ageing after homogenization practice is investigated through hardness measurements.



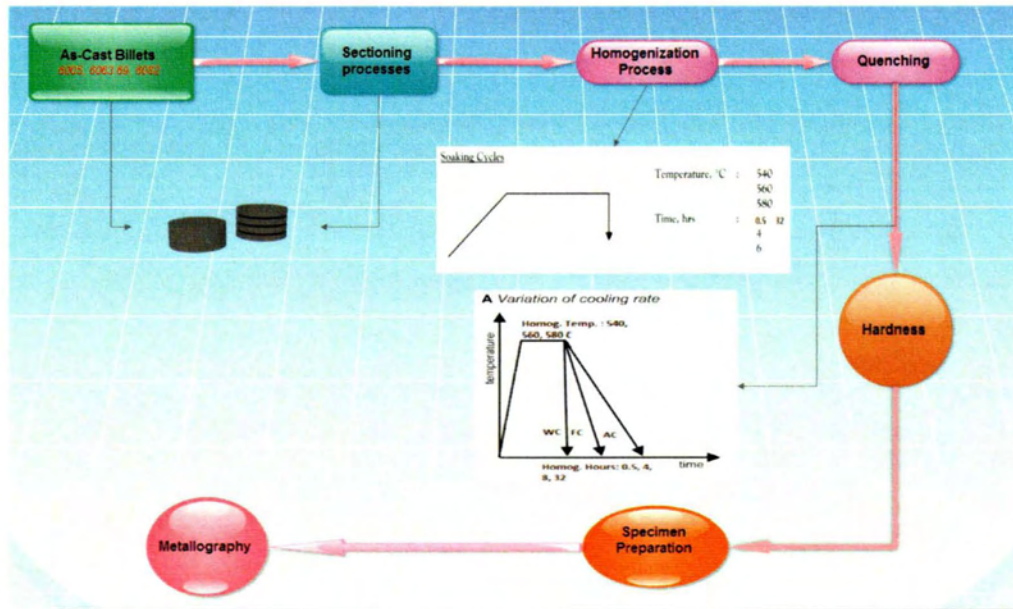
# Chapter 3

## Experimental Procedures

*All experiments and procedures performed in this dissertation, and how they were conducted, are described in detail on this chapter.*

### 3.1 Methodology and materials

A brief summary of the experimental procedure is given in the flowchart in **Figure 3.1**. Consecutively, the as-cast billets were sectioned in small specimens, homogenized and quenched, measured in hardness, properly prepared and finally investigated through optical microscopy.



**Fig 3.1** Experimental procedure - flowchart.

In the present study three aluminum alloys of industrial interest of the 6xxx series were investigated. Specifically the experimental work was conducted in 6082, 6005 and 6063. Alloys were provided in the as-cast state by the Aluminum of Greece (AoG) to the Laboratory of materials (LoM) of the University of Thessaly. The chemical compositions of the alloys are given in **Table 3.1** below.

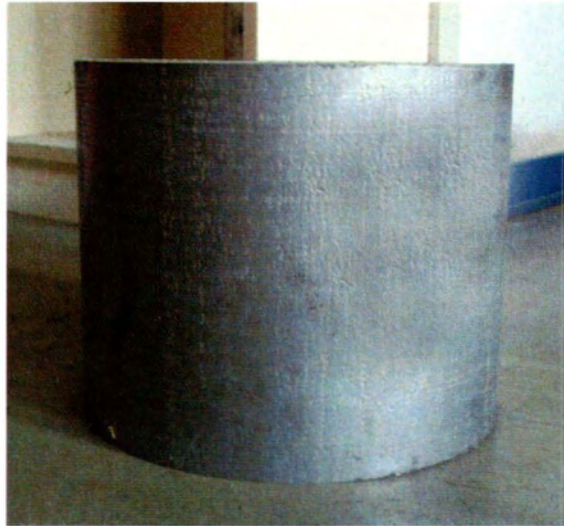
**Table 3.1** Chemical compositions of the aluminum alloys

A/A	Si	Fe	Cu	Mn	Mg	Cr	Others
6082	0.9 - 1.05	- 0.25	- 0.05	0.45 - 0.55	0.63 - 0.77		0.04
6005	0.5 - 0.55	0.18 - 0.22	- 0.02	0.032 - 0.042	0.5 - 0.55	- 0.01	0.02
6063	0.65 - 0.72	- 0.24	0.08 - 0.14	0.2 - 0.3	0.45 - 0.53	- 0.05	0.03

### 3.2 Sectioning

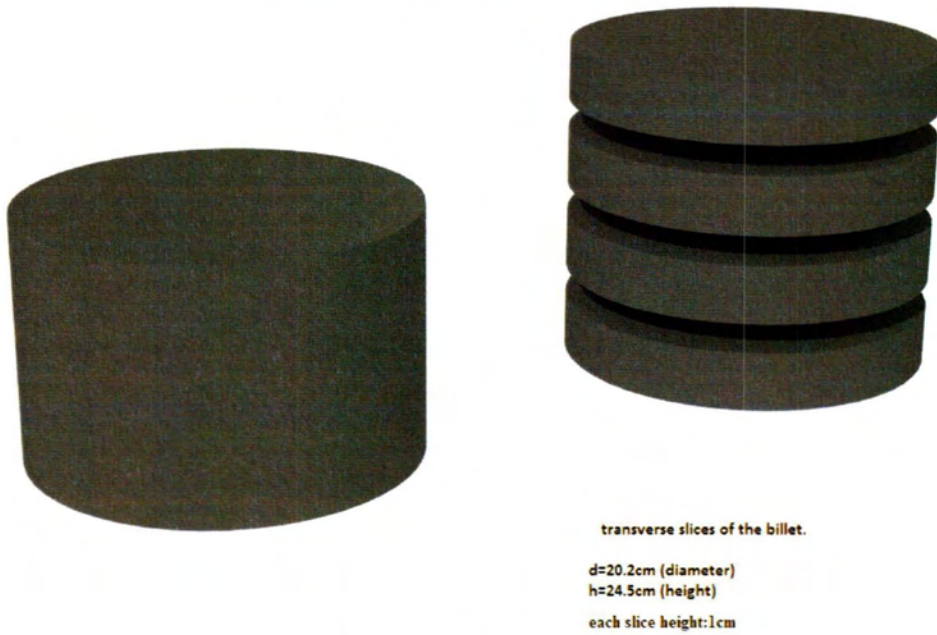
The received billets (**Figure 3.2**) were sectioned in transverse slices as shown in **Figure 3.3**. Then 108 samples of 10mm thickness were cut from approximately the middle of the billet's

slice radius in order to avoid edge inhomogenities and other casting defects. The 108 specimens were grouped in a way to be able to distinguish them. This grouping of the specimens is given in tables in **Appendix 2**.



**Fig.3.2** The aluminum billets as received.

**As cast billets sectioning**



**Fig 3.3** Billet's sectioning

### 3.3 Metallography

Specimen preparation included cutting and grinding with SiC papers rating 800, 1000, 2400 and 4000 grit. Polishing was performed with 3 and 1 $\mu$ m diamond paste followed by electro-polishing with Barkers reagent consisting of 10 milliliter fluoroboric acid (35 %) and 200 milliliter water. The microstructure was revealed after etching in Keller's solution, consisting of 0.5% HF in 50ml H<sub>2</sub>O in order to reveal and indentify the intermetallic phases. In order to study the microstructural evolution during the homogenization procedure the as-cast microstructure has been investigated through an optical microscope.

The volume fractions of the Mg<sub>2</sub>Si and  $\alpha$ + $\beta$  phases has been calculated, through quantitative methods using Photoshop and Image J software. The results were then compared with the corresponding results of the Thermo-Calc simulation of the solidification process of 6082 alloy. The as-cast microstructure has also been compared with the as-homogenized in order to study the addition of homogenization time and temperature as well as the cooling rates. Metallographic examination was carried out using an optical microscope.

### 3.4 Homogenization and quenching process

Homogenization heat treatments were performed on each of the 108 specimens that were taken after the sectioning process. The treatments were performed using a furnace available on the materials laboratory of the university. A type K thermocouple was used to identify that the furnace indication was the right one. The thermocouple was also used to measure the cooling rate of the specimens physically in the air and artificially with a fan.

The homogenization trials were performed for a constant heating rate of 560°C within 17 minutes by changing the soaking and cooling cycles. (Figure 3.4-3.5) The soaking experiments were in a temperature range of 540°C-580°C for 30min, 4hr, 6hr and 32 hr, while the samples were rapidly cooled in water (Q), physically in the air (AC) and artificially with a fan (FC). These parameters were chosen through the referred literature.(Table 3.2) The temperature range was selected so that to be between the solidus and solvus temperature and it is confirmed from the phase diagrams that has been extracted from Thermo-Calc software.

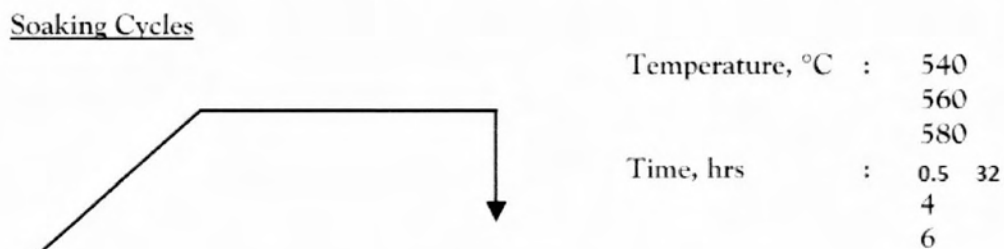
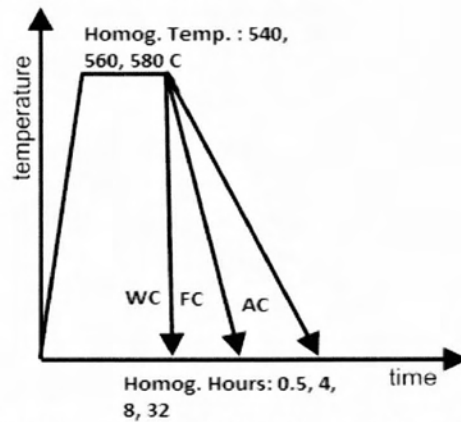


Fig. 3.4 Soaking cycles of the experimental procedure

**A Variation of cooling rate**



**Fig. 3.5** Cooling practice variation of the experimental procedure

**Table 3.2** A synopsis of the experimental parameters and its sources.

Time [=] hr	Temperature [=] °C	Cooling practice	Reference
0.5	540	Quenched (Q)	[1,2,23,25,27]
4	560	Forced Cooling (FC)	[1,2,23,25,27]
8	580	Air Cooling (AC)	[1,2,23,25,27]
32			[27]

### 3.5 Hardness measurements

Hardness tests were performed immediately after the homogenization process in order to investigate its effect on hardness. Moreover, hardness tests were performed after five days of the homogenization in order to study the natural aging effect on the materials. It has proven that the main increase on the hardness of aluminum 6xxx alloys is within the first five days after the thermal treatment. [30, 23]

Brinell macro-hardness test was applied in the specimens. It will be briefly mentioned that an indenter steel ball is pressed into the sample by an accurately controlled test force for a specific dwell time. The size of the indent is determined in different ways. We did it through Photoshop software, namely, the imprints were pictured in stereoscope and then the indents were measured. The Brinell hardness number is a function of the test force divided by the curved surface area indent and is given by the following equation:

$$HB = 0.102 * \frac{\text{Load}(N)}{\text{Surface Area of Indentation (mm}^2)} = 0.102 * \frac{2P}{\pi D[D - \sqrt{D^2 - d^2}]} \quad (3.1)$$

In the hardness test performed for the current experiment, it was used a 5mm diameter of indenter and a load of 250kg for 15 seconds. As mentioned above, the indentation diameter was calculated with Photoshop and the final HB number with an excel function.

# Chapter 4

## Results and Discussion

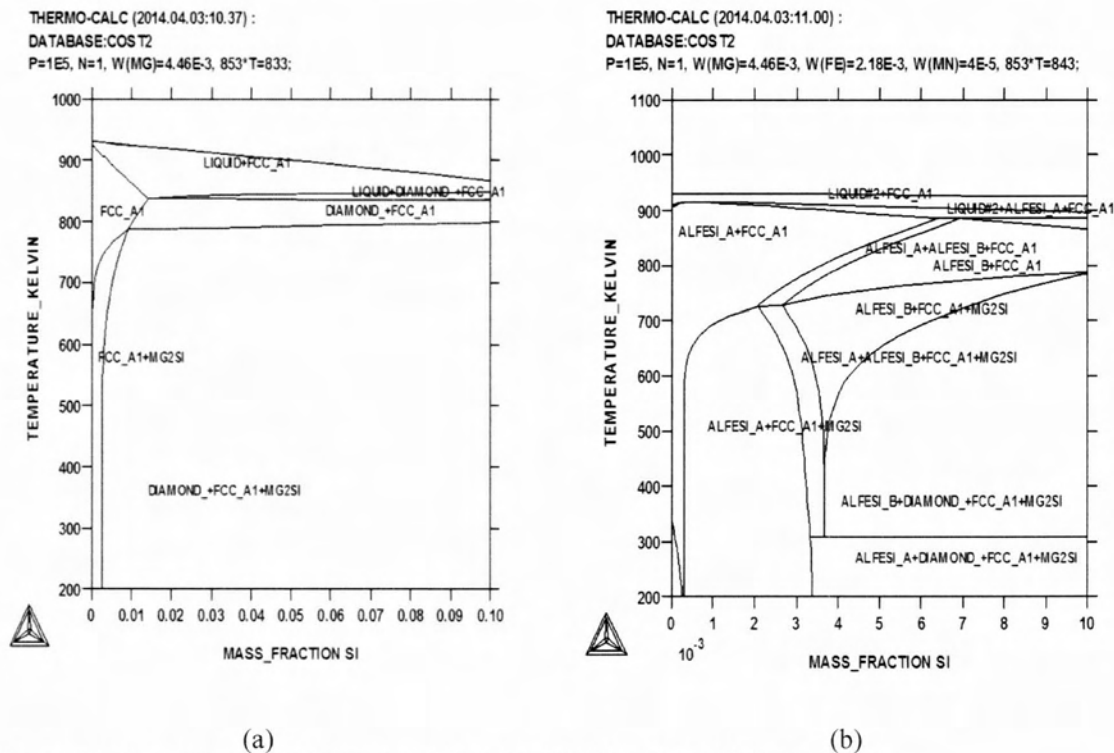
*In this chapter the results of the experiment described in the previous chapter will be presented. A discussion of the results will be performed taking into account the theoretical background presented in chapter 2.*

## 4.1 The as-cast microstructure

- **Computational Thermodynamics**

In order to determine the experimental homogenization temperature range, temperature-composition diagrams according thermodynamic equilibrium were performed with the Thermo-Calc software. These are temperature-composition diagrams, where the composition of one alloying element is allowed to vary within a specified range, while the composition of the remaining alloying elements is kept constant are depicted in **Figure 4.1**. One of the most comprehensive thermodynamic databases for aluminum alloys, and in general for light, non-ferrous alloys, is the COST 507 database. The major phases in the Al-Mg-Si-Fe-Mn system are Liquid phase, the FCC matrix phase ( $\alpha$ -Al), the intermetallic phases Mg<sub>2</sub>Si,  $\alpha$ -AlFeSi,  $\beta$ -AlFeSi and the Si-diamond phase.

These diagrams confirm that the temperature range used for the homogenization thermal treatment is a safe limit for the alloys because it is between the solvus and solidus curves.



**Figures 4.1** a) Ternary Al-Mg-Si system and b) an isopleth of the Al-Mg-Si-Fe-Mn system

However under high solidification rates (2mm/sec) employed in direct-chill casting operations in industry and assuming negligible diffusion in the solid state during casting, the composition profile of the alloying elements can be described with the Scheil equation:

$$c_s = c_0 k (1 - f_s)^{k-1} \quad (4.1)$$



Where,  $c_o$  is the alloy nominal composition,  $k$  the partition coefficient and  $c_s$  the composition when the solid mass fraction is  $f_s$ . It should be mentioned that equation 4.1 is valid for binary alloy systems. In our work, the microsegregation in the Al-Mg-Si-Fe-Mn system can not be described by equation 4.1. The description of microsegregation requires the application of computational thermodynamics, especially the Thermo-Calc software, which has I built in Scheil module.

A typical solidification path, using the Scheil module of Thermo-Calc, for a 6082 alloy with composition Al-0.63Mg-0.9Si-0.2Fe-0.45Mn (wt%) is shown in **Figure 4.2** as a temperature vs mass fraction of solid. The phase sequence during solidification is FCC $\rightarrow\alpha$ -AlFeSi $\rightarrow\beta$ -AlFeSi $\rightarrow$ Mg<sub>2</sub>Si $\rightarrow$ Si (diamond). The arrows show the temperature and the mass fraction of solid where each phase starts to form. The liquidus temperature for this alloy was calculated to be 651°C and the solidus temperature is 548°C.

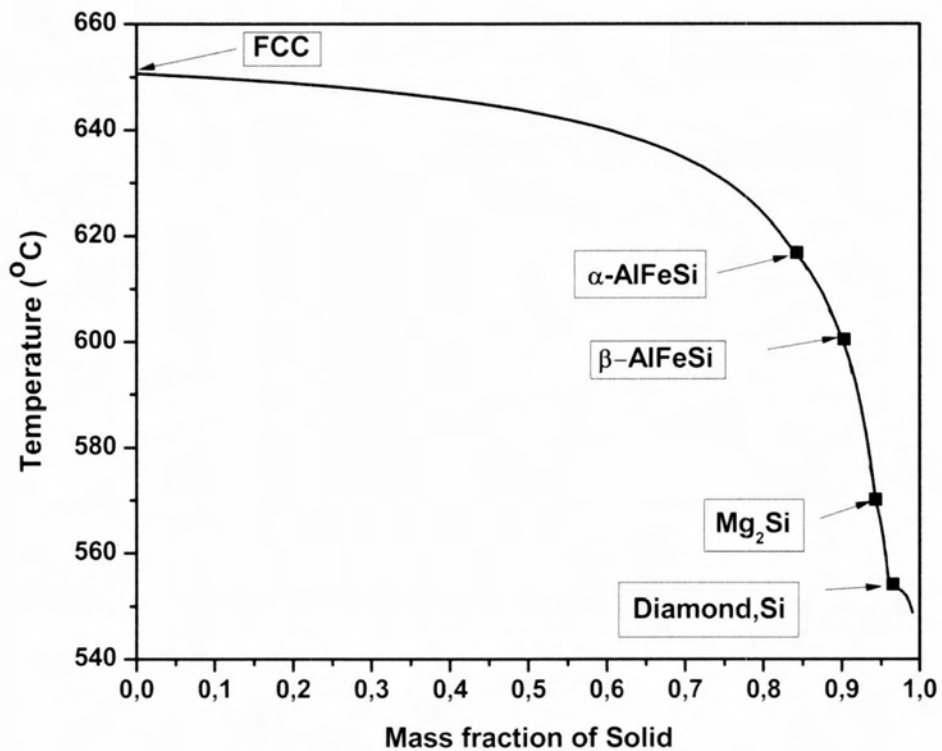


Fig.4.2 Solidification path of AA6082

## 4.2 Metallographic observations – Optical microscopy

### 4.2.1 As-cast microstructure

A typical as-cast microstructure of 6082 alloy is depicted in Fig.4.3 where the microstructure is consisted of aluminum dendrites and an interdendritic network of the Al-Fe-Si particles in a magnification of X500. As illustrated in Fig. 4.4 the microstructure is consisted of the strengthening phase  $Mg_2Si$  (black), the intermetallics,  $\alpha-AlFeSi$  and  $\beta-AlFeSi$  phases with a light grey and a dark grey color respectively and shown with arrows.

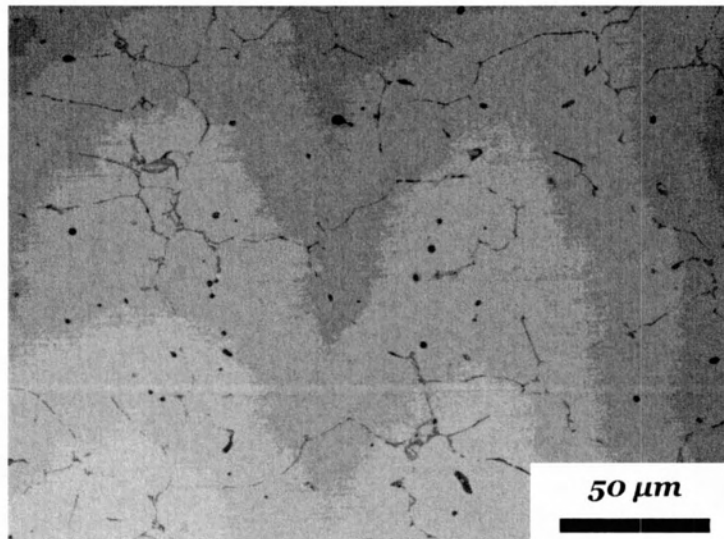


Fig 4.3 Interdendritic network of aluminum 6082

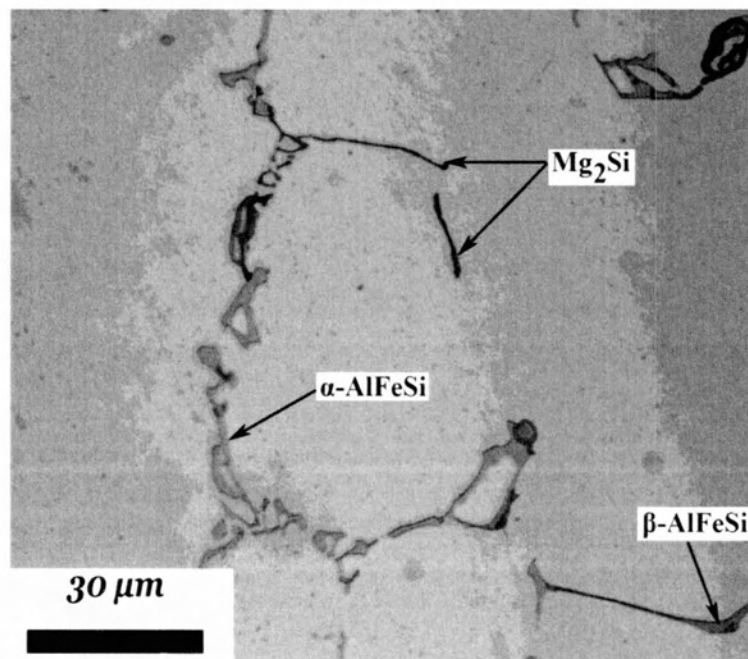


Fig. 4.4 Microstructure special characteristics of 6082

In addition, in **Figures 4.5-4.6** some specific characteristics of the microstructure such as the typical “Chinese script” of the  $\alpha$ -AlFeSi and the eutectic structure are also shown in a higher magnification of x1000. The eutectic structure as referred to the literature is consisting of FCC +  $\beta$ -AlFeSi + Mg<sub>2</sub>Si + Si. On higher magnification it is obvious the distribution of the  $\alpha$ -AlFeSi and  $\beta$ -AlFeSi phases connected sometimes with Mg<sub>2</sub>Si on the grain boundaries. Finally, it has to be mentioned that the separation between the  $\beta$ -AlFe(Mn)Si and  $\alpha$ -AlFe(Mn)Si was impossible through optical microscopy.

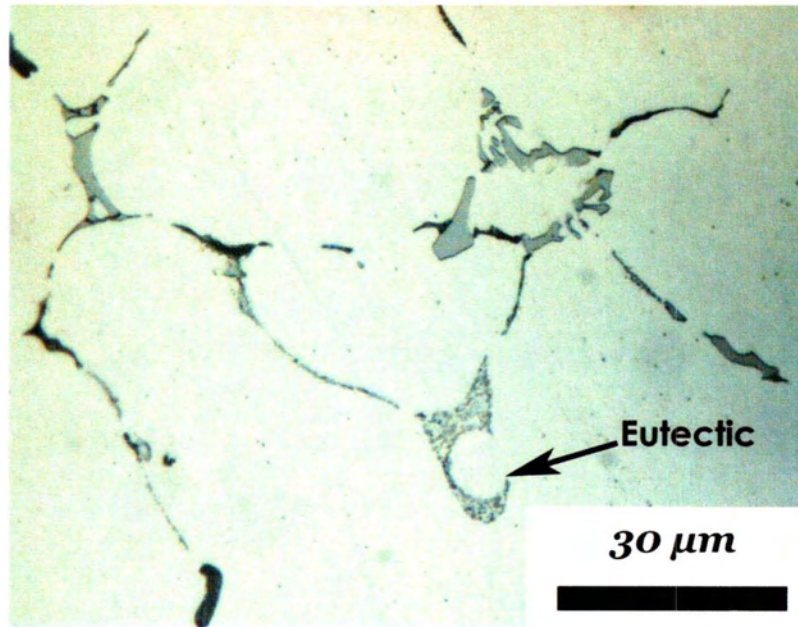


Fig. 4.5 Eutectic structure

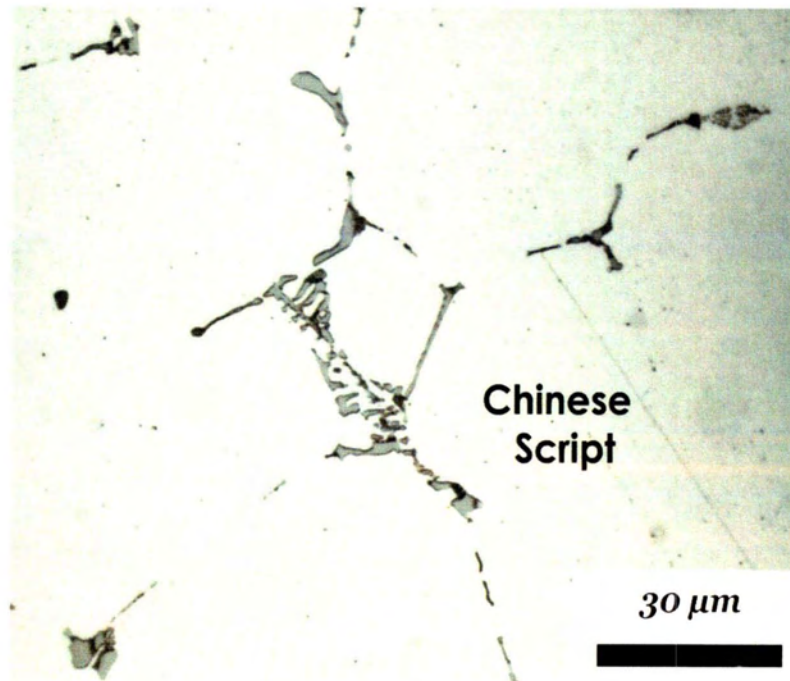


Fig. 4.6 Chinese Script

## 4.2.2 Validation of the volume fractions of intermetallic phases

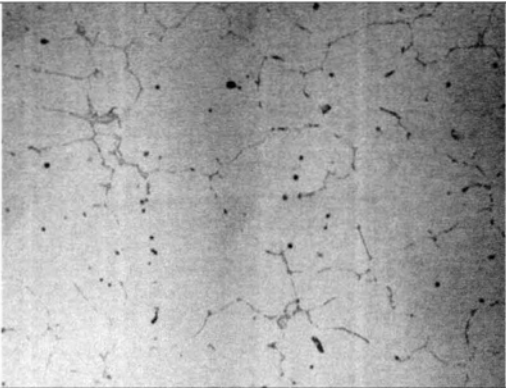
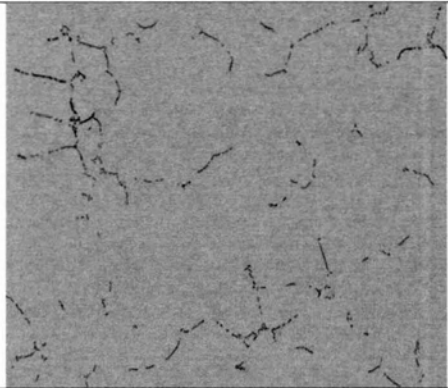

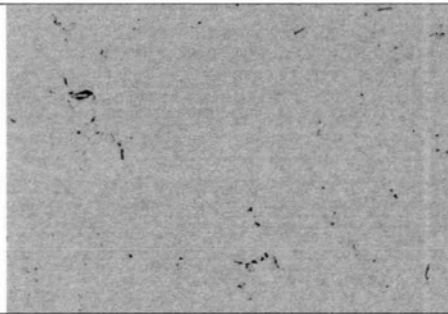
Subsequently after metallographic examination of the as-cast microstructure, quantitative methods in order to calculate the volume fractions of the  $Mg_2Si$  and  $\alpha+\beta$  phases, were applied. According to a simulation of the solidification process of 6082 aluminum alloy as discussed above the volume fractions of the  $Mg_2Si$  and  $\alpha+\beta$  phases were validated to those of the quantitative method.

Regarding the  $Mg_2Si$  fractions, the simulation and the quantitative method results are in a good agreement. However, the results for the  $\alpha+\beta$  phases show significant differences.

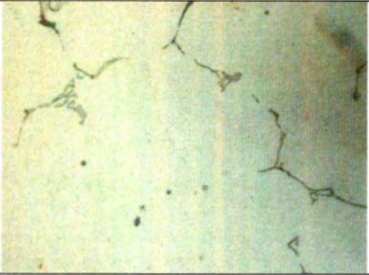


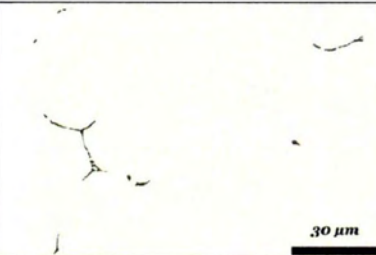
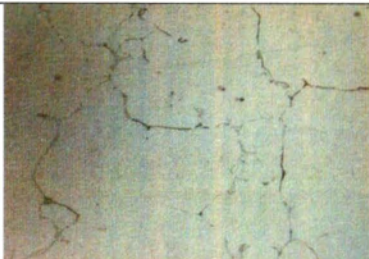

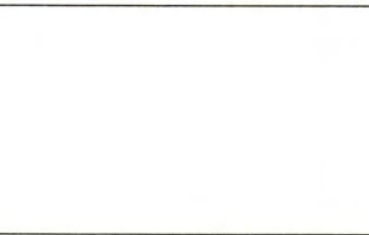
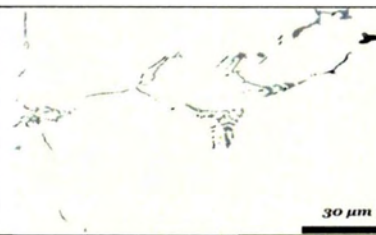
The exact\*<sup>1</sup> microstructure was visible under high magnification of the X500 magnitude. As a result, four consecutive photos were taken and then merged with Photoshop in order to take a representative area fraction of the alloy. On **Table 4.1** the results of this quantitative calculation are given, while on **Table 4.2** it is represented the results of the same calculations for the  $Mg_2Si$  phase fraction extracted from other images. However, the results are based only in one micrograph. For more exact volume fraction measurements more micrographs are needed in order to get statistically valid results. This work was not in the objections of the present thesis.

\*1) Using the term "exact microstructure" we mean, to be able to distinguish and measure the  $Mg_2Si$  and  $\alpha+\beta$  phase

Table 4.1 Quantitative calculations of a merged photo (X500)

No	Photo	Magnification	Area Selected for Calculation	Phase	Calculation Software	Area, $\mu\text{m}^2$	Total Area, $\mu\text{m}^2$	%	Scheil	
1.		X500		Mg2Si	Photoshop	146,484	43355,59	0,337	0.385	
					ImageJ	141,796				0,327
					<b>Average: 0,332</b>					
2.		X500		$\alpha+\beta$	Photoshop	97,79	43355,59	0,225	0.42	
					ImageJ	91,95				0,212
					<b>Average: 0,218</b>					

**Table 4.2** Additional quantitative measurements

No.	Photo	Magnification	Area Selected for Calculation	Phase	Calculation Software	Area [=] $\mu\text{m}$	Total Area, $\mu\text{m}^2$	Percentage %
1.		X1000		Mg <sub>2</sub> Si	Photoshop	48,639	12132,016	0,40
					ImageJ	40,449	12132,016	0,333
							<b>Average: 0,366</b>	
2.		X1000		Mg <sub>2</sub> Si	Photoshop	48,111	12132,016	0,396
					ImageJ	42,766	12132,016	0,353
							<b>Average: 0,374</b>	
3.		X500		Mg <sub>2</sub> Si	Photoshop	156,074	43355,59	0,359
					ImageJ	154,880		0,361
							<b>Average: 0,360</b>	
4.		X1000		Mg <sub>2</sub> Si	Photoshop	43,234	12132,016	0,356
					ImageJ	40,228	12132,016	0,332
							<b>Average: 0,344</b>	

### 4.2.3 Time evolution of the microstructure of 6082 during homogenization

The cooling rates measured with a type K thermocouple are presented on the diagram below (Figure 4.7). It was found that the specimens cooled naturally in the air need about 6 minutes to reach 150°C, while the specimens cooled with a fan need 2.5 minutes to reach the 150°C. It has to be mentioned that a temperature limit of the 150°C was used, because below that temperature no microstructural change occurs.

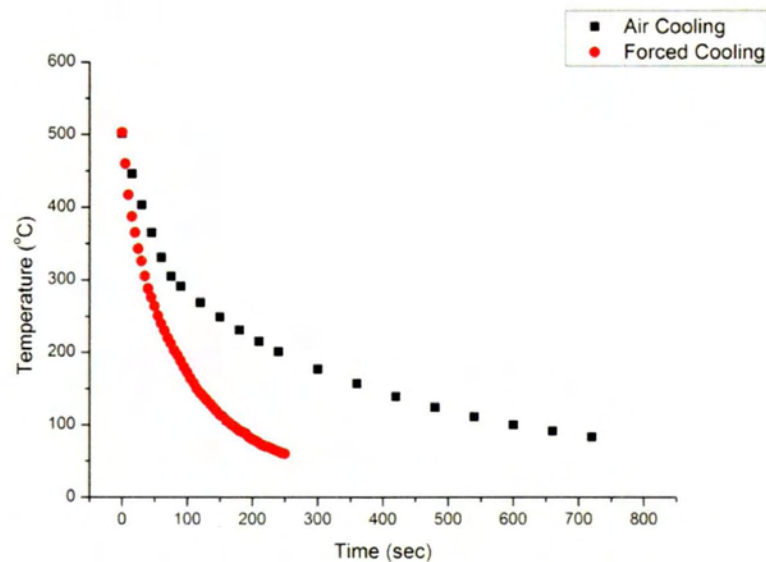


Fig.4.7 Cooling rates – Air Cooling (AC), Forced Cooling (FC)

Figures 4.8 and 4.9 illustrate the microstructures of those samples that were soaked between 540 and 580°C for 0.5, 4, 8 and 32 hours and subsequently air cooled and water quenched, respectively for the 6082 aluminum alloy. Soaking at 540°C, 560°C and 580°C for 30 minutes seemed to have produced little change in the type and distribution of the intermetallic phases. There was no change in the morphology of the interdendritic particles and the transformation of the  $\beta$ -AlFe(Mn)Si to  $\alpha$ -AlFe(Mn)Si was insignificant.

In contrast, there were considerable morphological and microstructural changes starting at 4 hours of soaking. These changes are more evident as the temperature and homogenization time increases. The  $\beta$  phase started to break up into small discrete particles at soaking time up to 4 hours.

Taking a closer look at these figures it is obvious that the microstructural changes are more prominent at 580°C. After a homogenization time of 8 hours the interdendritic platelets were replaced almost entirely of discrete round particles. This distribution is called ‘‘necklace’’ configuration and it is likely the  $\beta$ -AlFeSi phase has completely transformed to the  $\alpha$ -AlFeSi.

Techniques other than optical microscopy have to be applied in order to identify this transformation, such as EDS and XRD. A first estimation may be performed based on the morphology of the phases. As it is known the  $\beta$  particles edges are sharper than the edges of the  $\alpha$  phase which are more rounded. With decreasing the homogenization temperature, these changes are obviously delayed. So it is confirmed that the  $\beta$ -AlFe(Mn)Si to  $\alpha$ -AlFe(Mn)Si transformation which is a diffusive transformation controls the time of homogenization procedure.

In addition the as-homogenized microstructure is strongly depended on soaking temperature and time. Regarding the Mg<sub>2</sub>Si phase, it is frequently observed that the Mg<sub>2</sub>Si distribution in the air cooled specimens is more uniform than the quenched in water specimens. That is because the specimens cooled naturally in air remain longer time at higher temperatures and as a result there is more time for the Mg<sub>2</sub>Si particles to distribute in the microstructure.



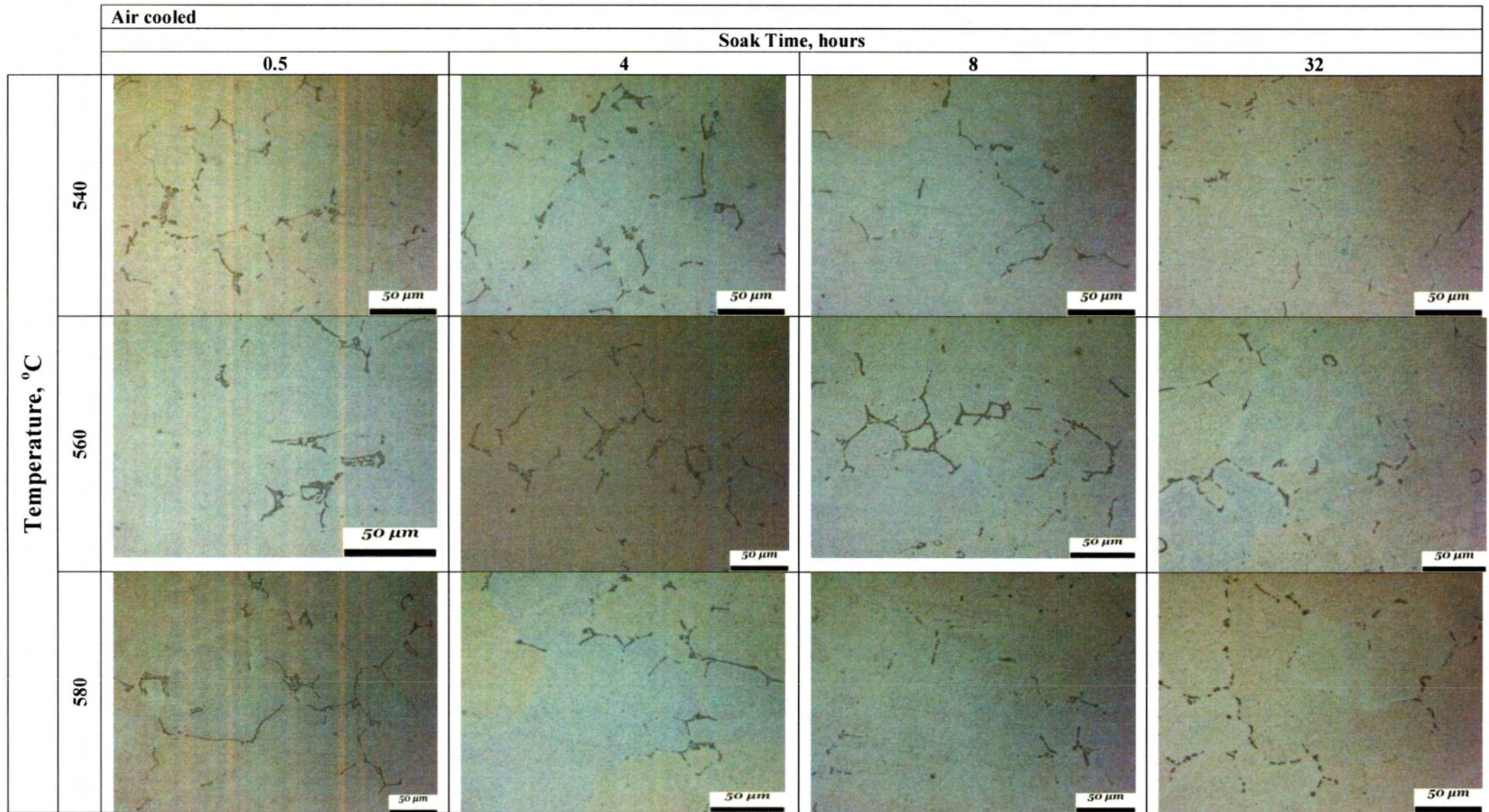


Fig. 4.8 The microstructural features of samples soaked between 540 and 580°C for 30min to 32 hours and subsequently air cooled.

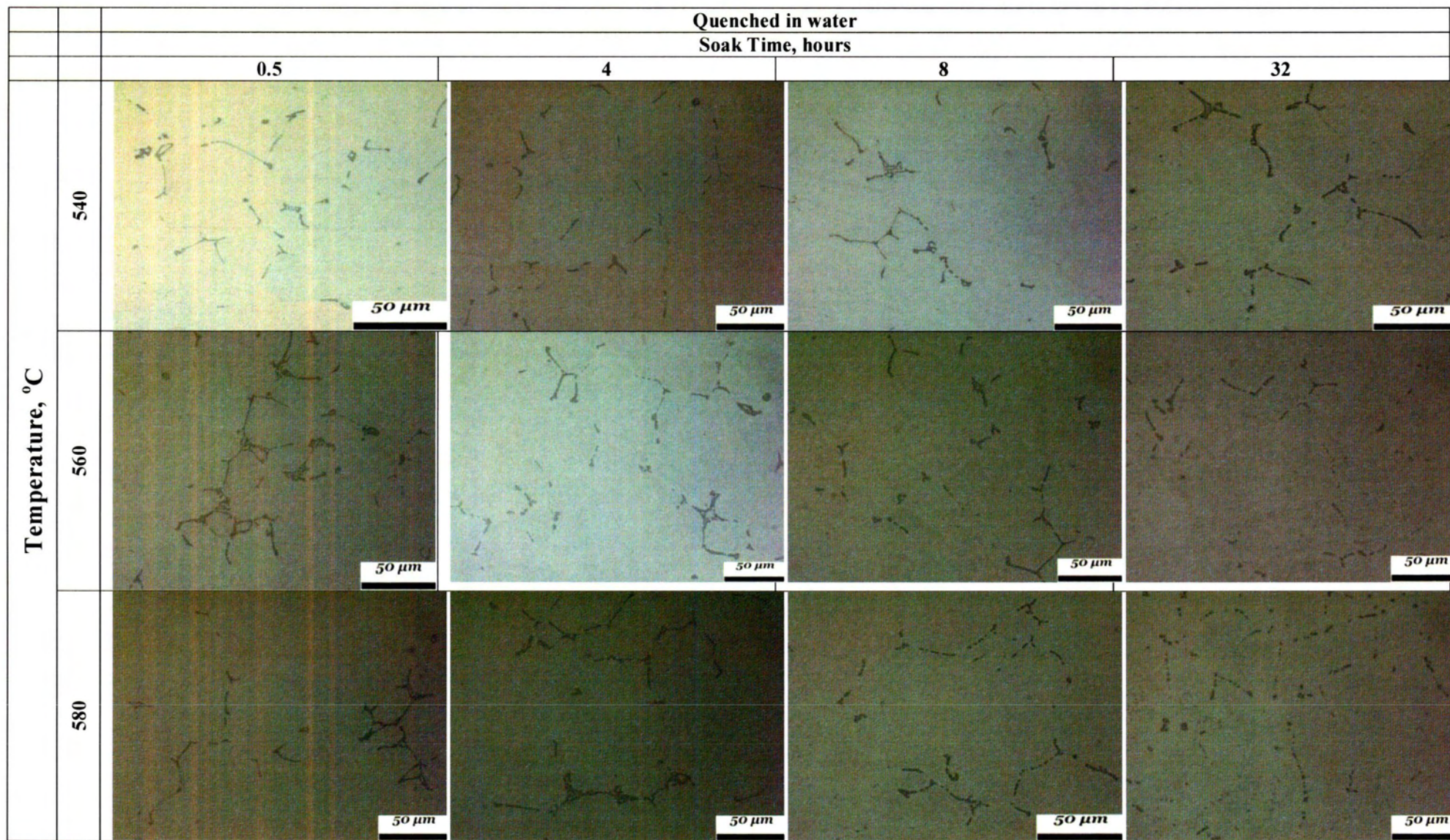


Fig. 4.9 The microstructural features of samples soaked between 540 and 580°C for 30min to 32 hours and subsequently quenched in water.

### 4.3 Hardness measurements - Immediately after homogenization and after natural ageing

Directly after the homogenization thermal treatment the Brinell hardness of the samples of the three alloys, 6082, 6005, 6063, were measured. The purpose of this was to study the effect of the homogenization time and temperature and the cooling rate on the hardness of the samples.

There are two main strengthening mechanisms taking place in these alloys which are reflected on the diagrams that follow. These are solid solution hardening and age/precipitation hardening.

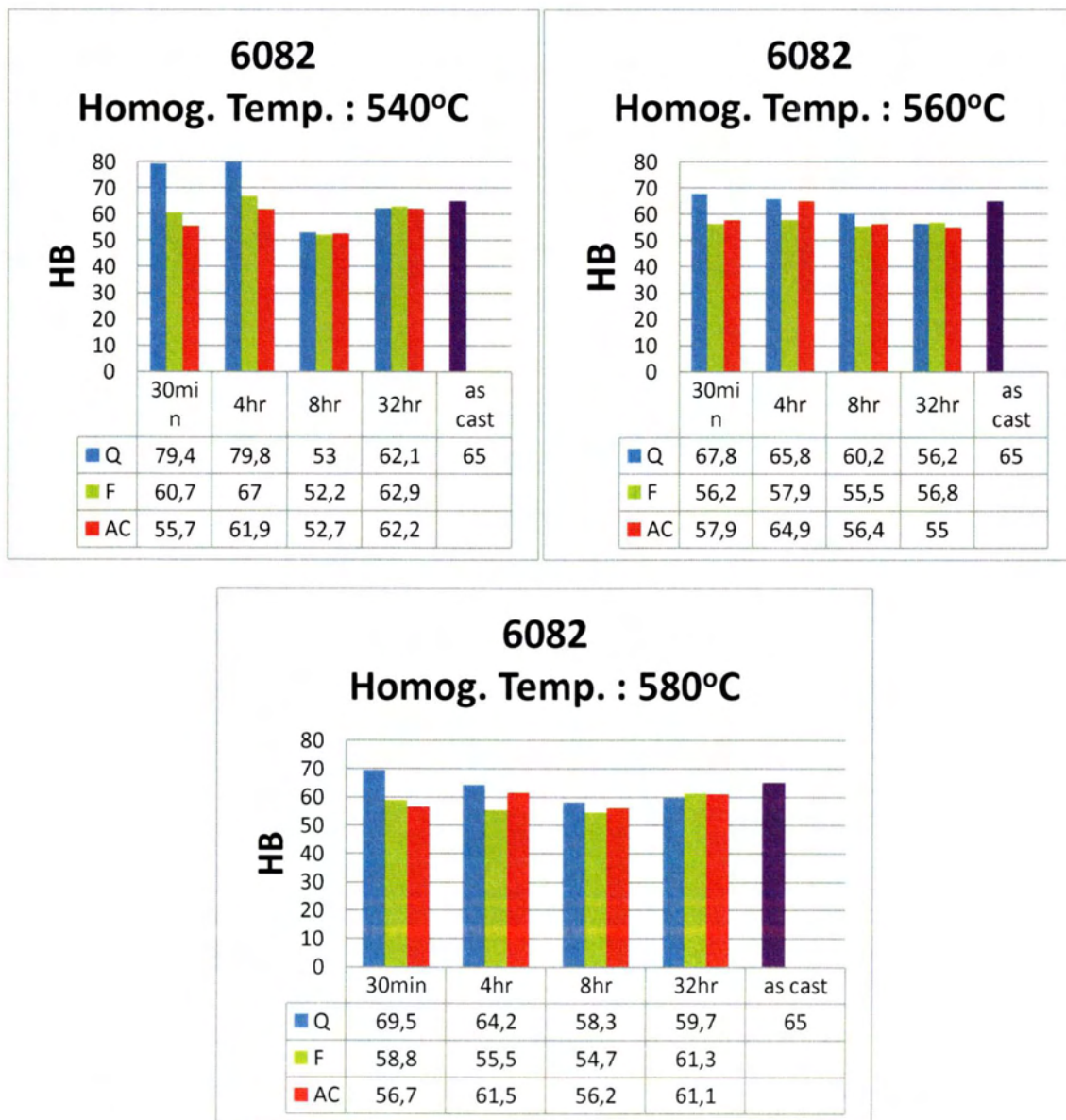


Fig.4.10 6082 after homogenization (AH) Brinell hardness, a) at 540oC, b) at 560oC and c) at 580oC

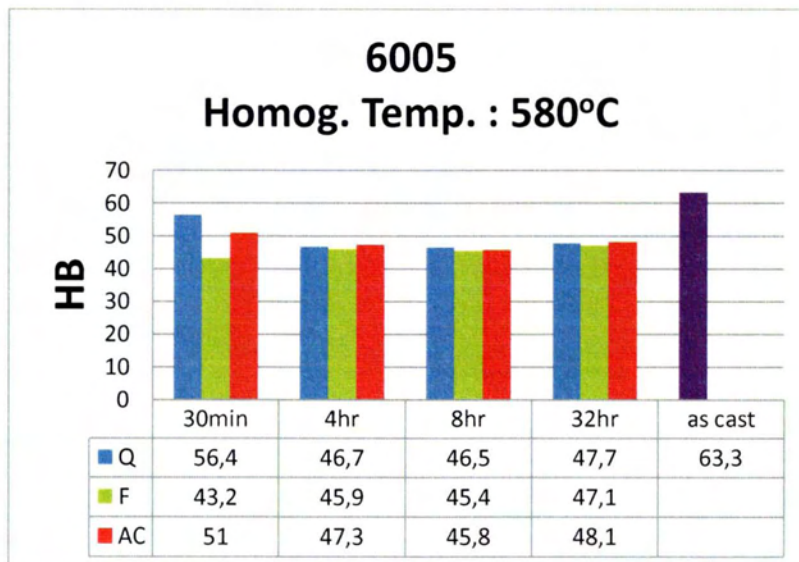
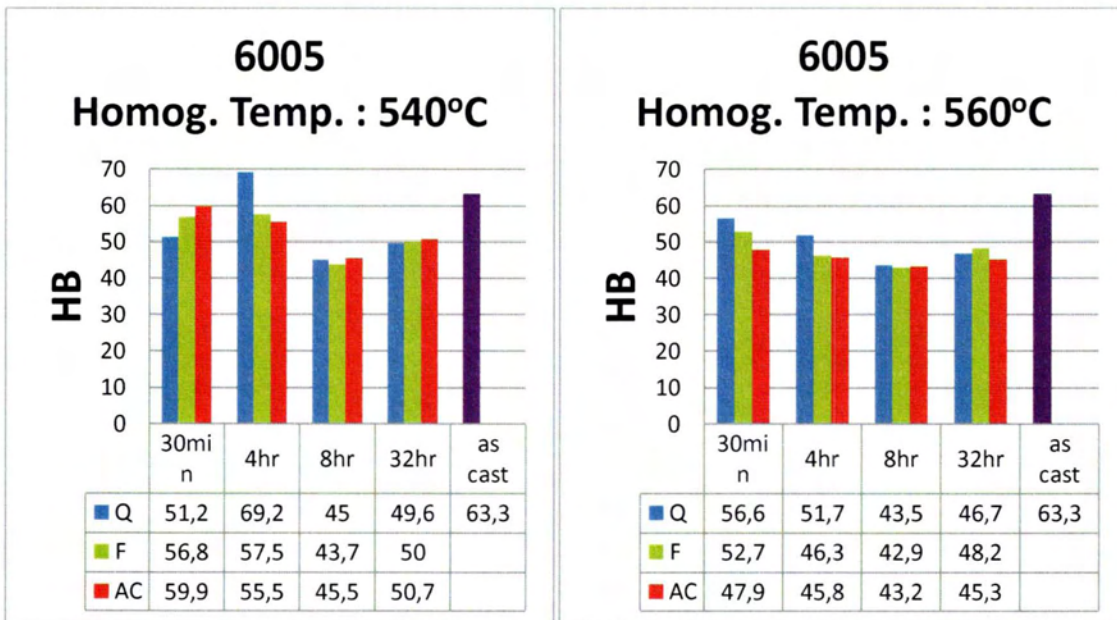


Fig.4.11 6005 after homogenization (AH) Brinell hardness, a) at 540oC, b) at 560oC and c) at 580oC

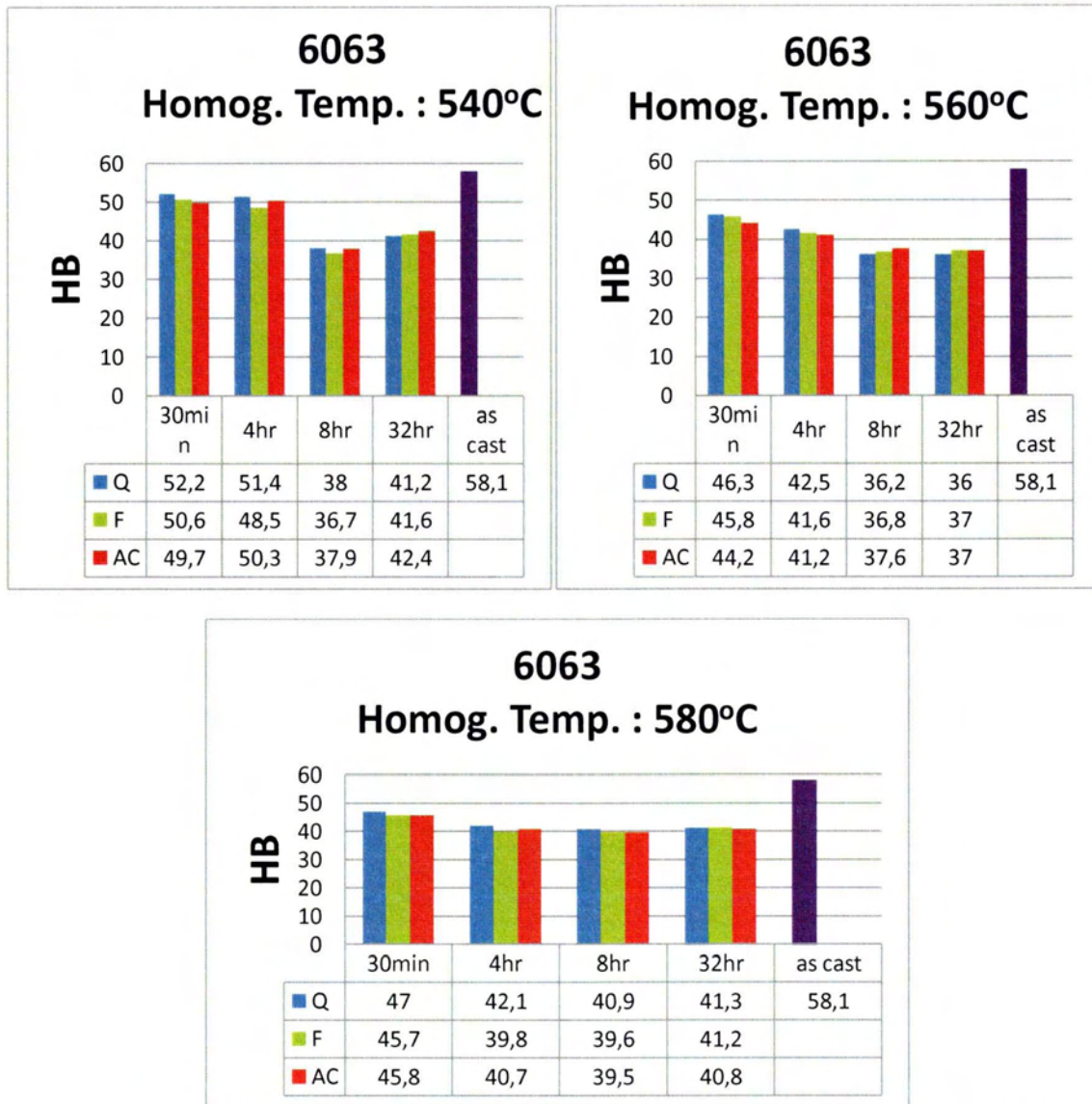


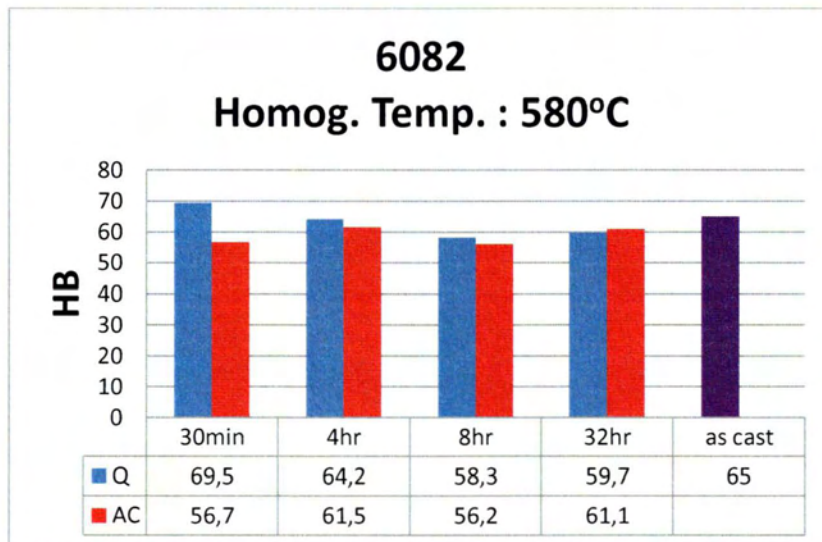
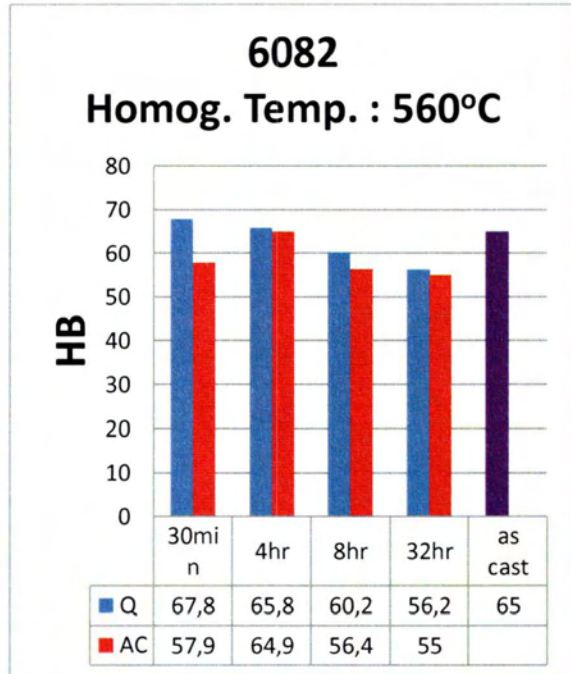
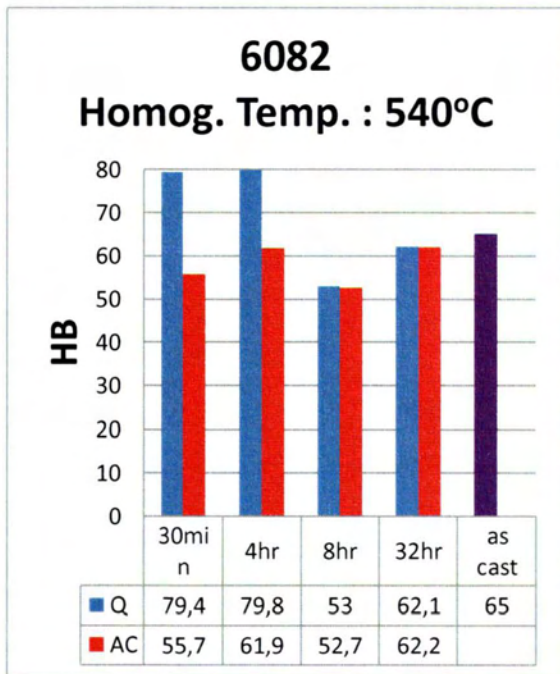
Fig.4.12 6063 after homogenization (AH) Brinell hardness, a) at 540oC, b) at 560oC and c) at 580oC

Taking a closer look on Fig. 4.10, about 6082 alloy, it is obvious the solid solution strengthening on the water cooled samples (blue columns). Due to the higher Mg and Si compositions of the 6082 alloy it is obtained higher amount of Mg<sub>2</sub>Si after solidification. Following the homogenization treatment, the objective of quenching is to preserve the solid solution formed at the soaking temperature, by rapidly cooling at room temperature. During rapid cooling in water the Mg and Si components are trapped in solution with little or no Mg<sub>2</sub>Si precipitation and the sample is characterized by a supersaturated solid solution, which strengthens the alloy. The same phenomenon takes place in the interaction between the non-symmetrical field, caused by the vacancy disks, and the dislocations. The vacancies are multiplied during homogenization and are trapped into the lattice after quenching. This phenomenon also strengthens the aluminum and both of them are illustrated in the 6082 column charts.(Fig 4.10) Regarding the 6082 alloy, it is observed a tendency the water quenched specimens to provide the highest hardness, the forced cooled specimens the lowest,

while the air cooled give an intermediate hardness. The highest strength of the rapidly cooled samples is due to the solid solution strengthening as explained above. Examining the forced cooled and the air cooled specimens (the green and the red columns respectively) it is understood why the higher brinell values are taken for the air cooled one's. By decreasing cooling rates the alloy remains for longer times at higher temperatures, so there is more time for the elements to diffuse into the solution. It could be said that the Mg<sub>2</sub>Si particles inside the dendrites increased with decreasing cooling rate and it is represented on **Fig.4.10** on the hardness of the air cooled specimens compared to those that were cooled on the ventilator.

Regarding the 6005 and 6063 alloys, the effect of diffusion kinetics on the homogenization treatment is evident. The homogenization process involves holding the metal at an elevated temperature for a sufficient time to allow the concentration gradients to diminish to an acceptable level. The controlling factor is thus the diffusivity of the alloying elements dictating the speed at which mass transfer may occur. For lower temperatures (e.g. 540°C), appreciable changes on the hardness are given on the transition of the 4 to 8 hour homogenization, while on higher temperatures appreciable changes are taken on the transition of 30 min to 4 hour homogenization. (**Fig.4.11-12**) It can be seen that the overall hardness values taken from 6005 and 6063 alloys are lower than these taken from 6082 and this is attributed on the lower Mg and Si compositions. Smaller percentages of Mg<sub>2</sub>Si particle are formed after solidification.

Another comment that should be done is that the specimens which were cooled naturally in the air (AC) and those cooled by a ventilator (forced cooling - FC) did not show any considerable difference in hardness. That is because the cooling rates were relatively very close to have significant changes in the hardness and microstructure. As a result, the columns about the forced cooled samples were extracted from the charts. (**Figures 4.13-15**) In addition, the difference in hardness between the samples quenched in water (Q) and those cooled naturally in the air (AC) is most evident in the lower homogenization times, 30minutes – 4 hours, and is closely related to the alloying levels of Mg and Si. Namely, this difference increases as the Mg and Si compositions increase. (6063 → 6005 → 6082) Moreover, with increasing Mg and Si compositions the hardness increases for a specific cooling rate. **Figures 4.16-18** compares the three alloys at a specific homogenization time and temperature and confirm the fact discussed above.



**Fig.4.13** 6082 after homogenization (AH) Brinell hardness – without the forced cooling columns

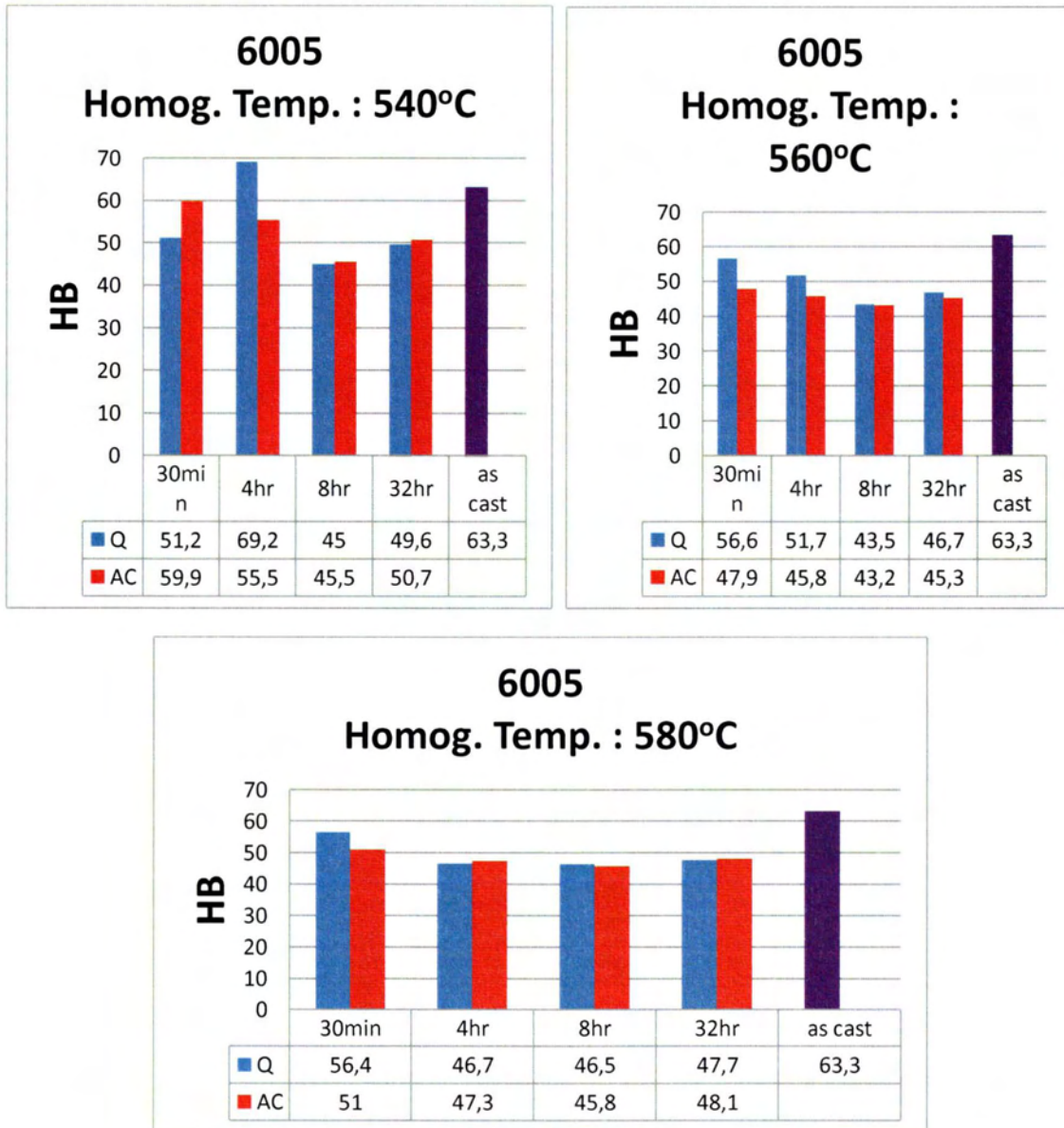
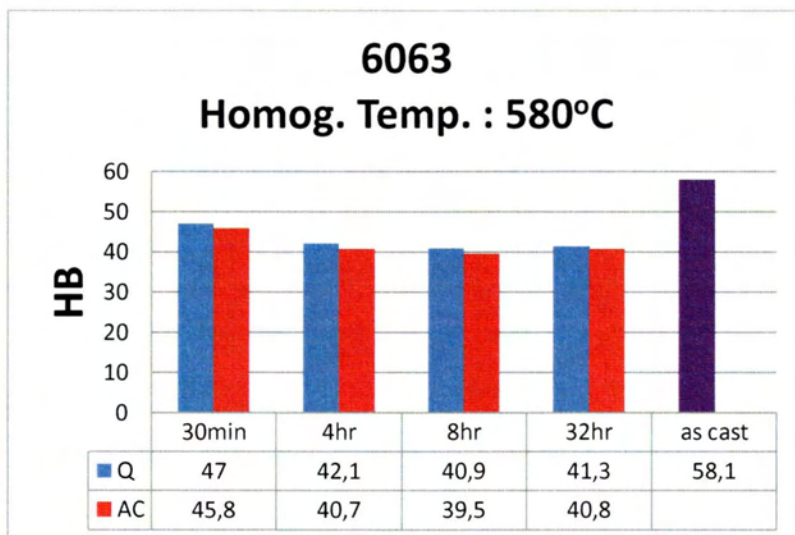
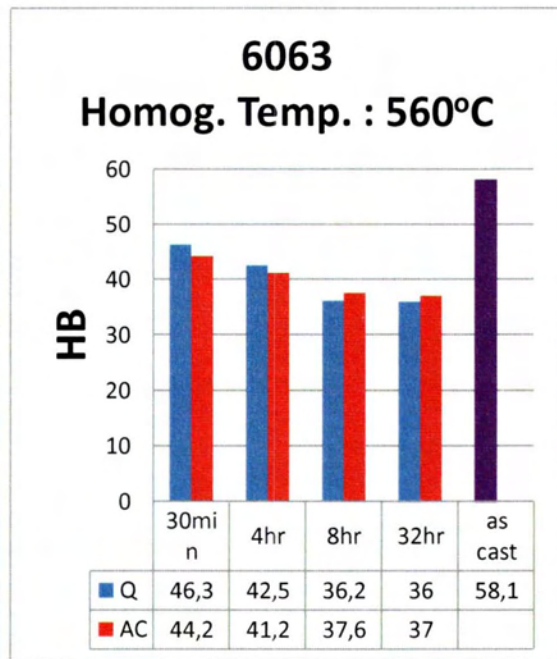
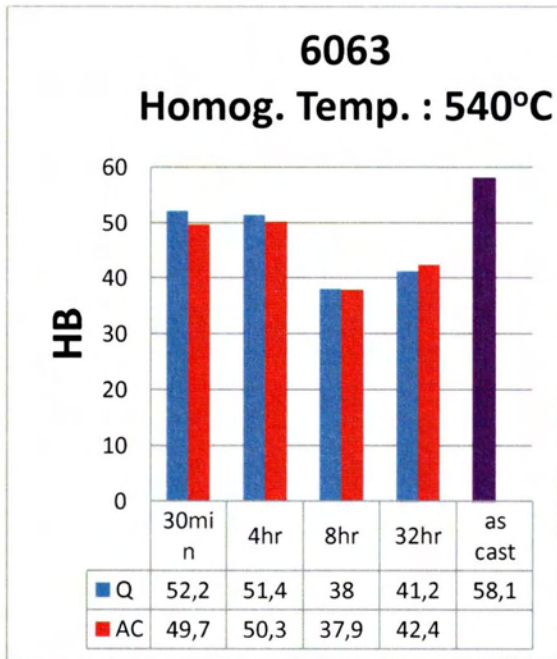


Fig.4.14 6005 after homogenization (AH) Brinell hardness – without the forced cooling columns





**Fig.4.15** 6063 after homogenization (AH) Brinell hardness – without the forced cooling columns

### Comparison of the alloys at 540°C for 4hours of homogenization

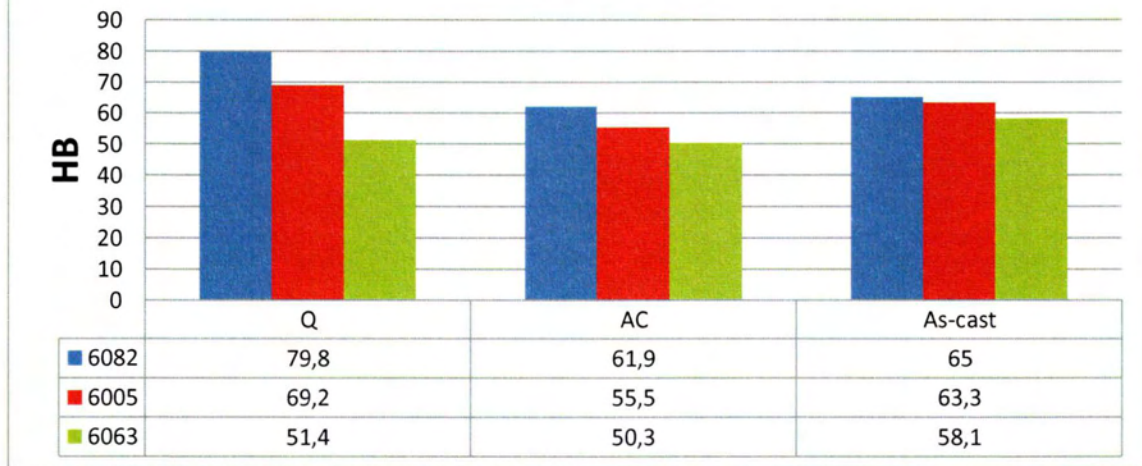


Fig. 4.16 Comparison of the 6082, 6005 and 6063 alloys at 540° C for 4hours of homogenization

### Comparison of the alloys at 560°C for 4hours of homogenization

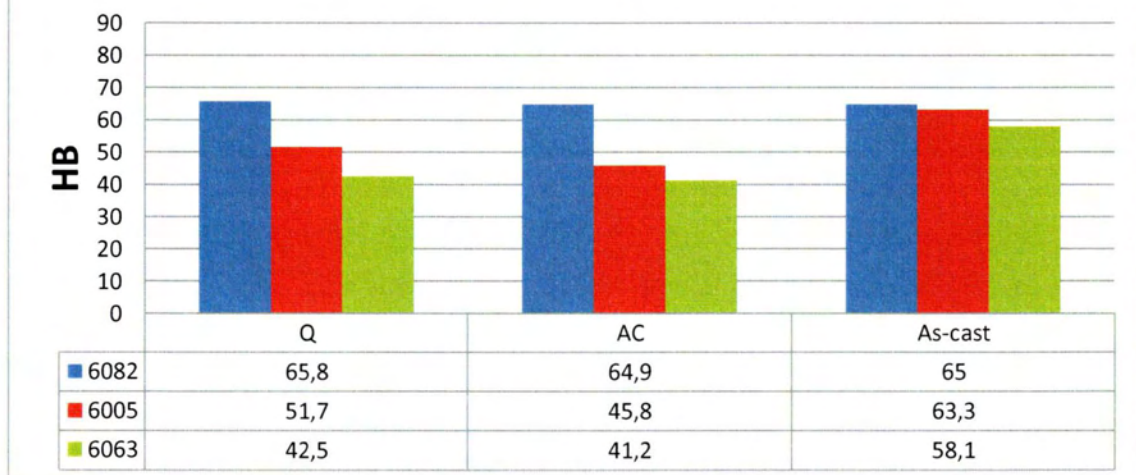
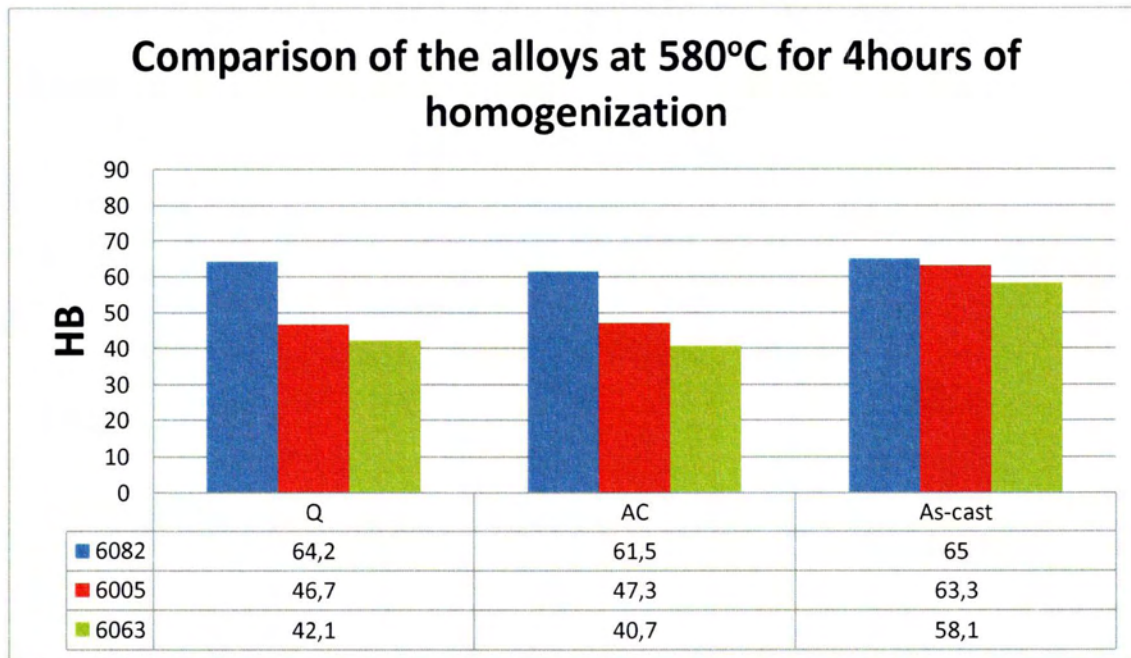


Fig. 4.17 Comparison of the 6082, 6005 and 6063 alloys at 560°C for 4hours of homogenization



**Fig. 4.18** Comparison of the 6082, 6005 and 6063 alloys at 580°C for 4hours of homogenization

It can be seen that the hardness is influenced even for an 8hr soaking, although the Mg and Si composition gradients are zero. This is because diffusion of the Mg and Si elements does not only depend on its composition gradients, but it is owed to the chemical potential gradients of other elements such as Fe, Mn which are not zero. Moreover, a slight increase in hardness is observed on the transition of the 8 to 32 hours of soaking. It is attributed either to the detained dissolution of the quaternary eutectics or to the various morphology of the Mg<sub>2</sub>Si particles. Larger particles dissolve in higher homogenization times. Homogenization is a thermal treatment where many diffusive transformations occur. As a result it is obvious the strong correlation among the temperature and the transformations during homogenization. Higher temperatures lead to faster transformations. The above explains the normalized hardness measurements taken for 580°C. For a homogenization temperature of 540°C, time is such a crucial parameter. We could say that the 540°C is a representative temperature in order to study the homogenization treatment. It was also observed that the alloys with low Mg and Si levels, 6005 and 6063, gave almost identical Brinell hardness numbers for temperatures 560 and 580°C. It could be a part of extra research to apply the same experiment but using lower homogenization temperatures for these alloys.

The samples were also investigated on their natural ageing potential. The process of natural ageing in alloy 6082 began almost instantaneously after homogenization heat treatment. Through bibliography it was found that within 5 days the 6xxx series aluminum alloys obtain their max hardness in terms of natural ageing. The graphs below represent the natural ageing (NA) Brinell hardness of the samples:

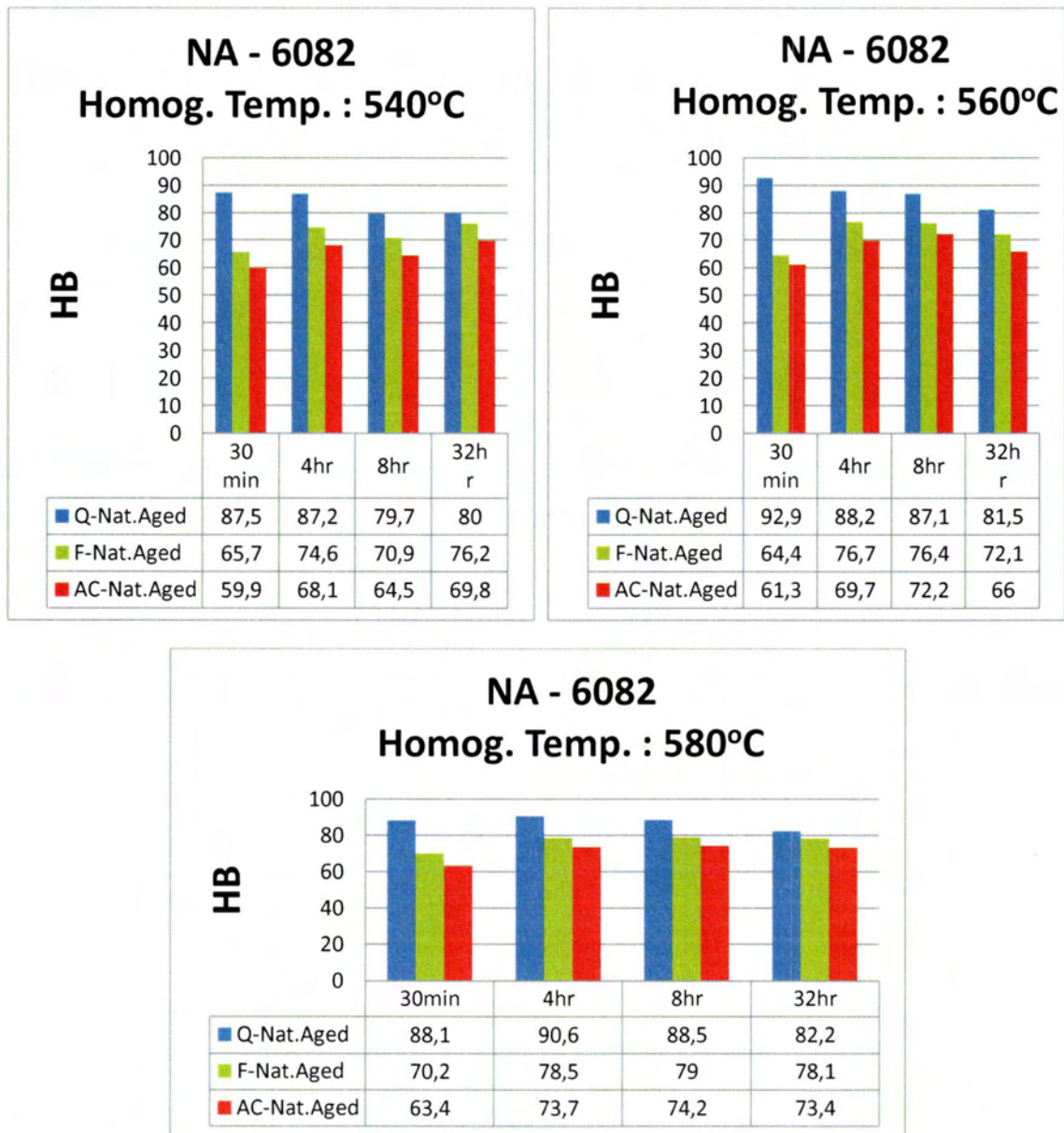


Fig.4.19 6082 Brinell hardness of the natural aged samples (NA) homogenized, a) at 540oC, b) at 560oC and c) at 580oC

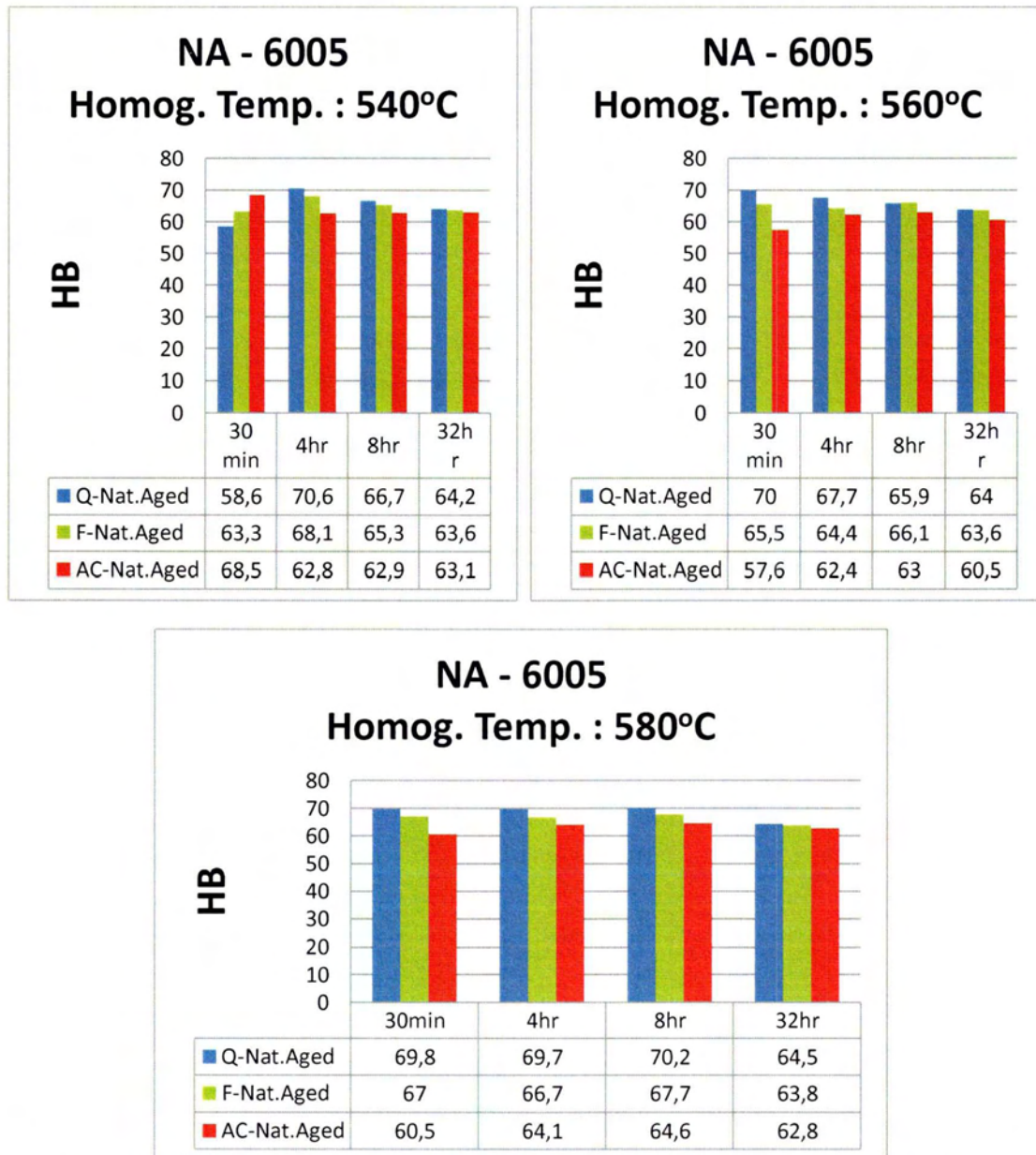
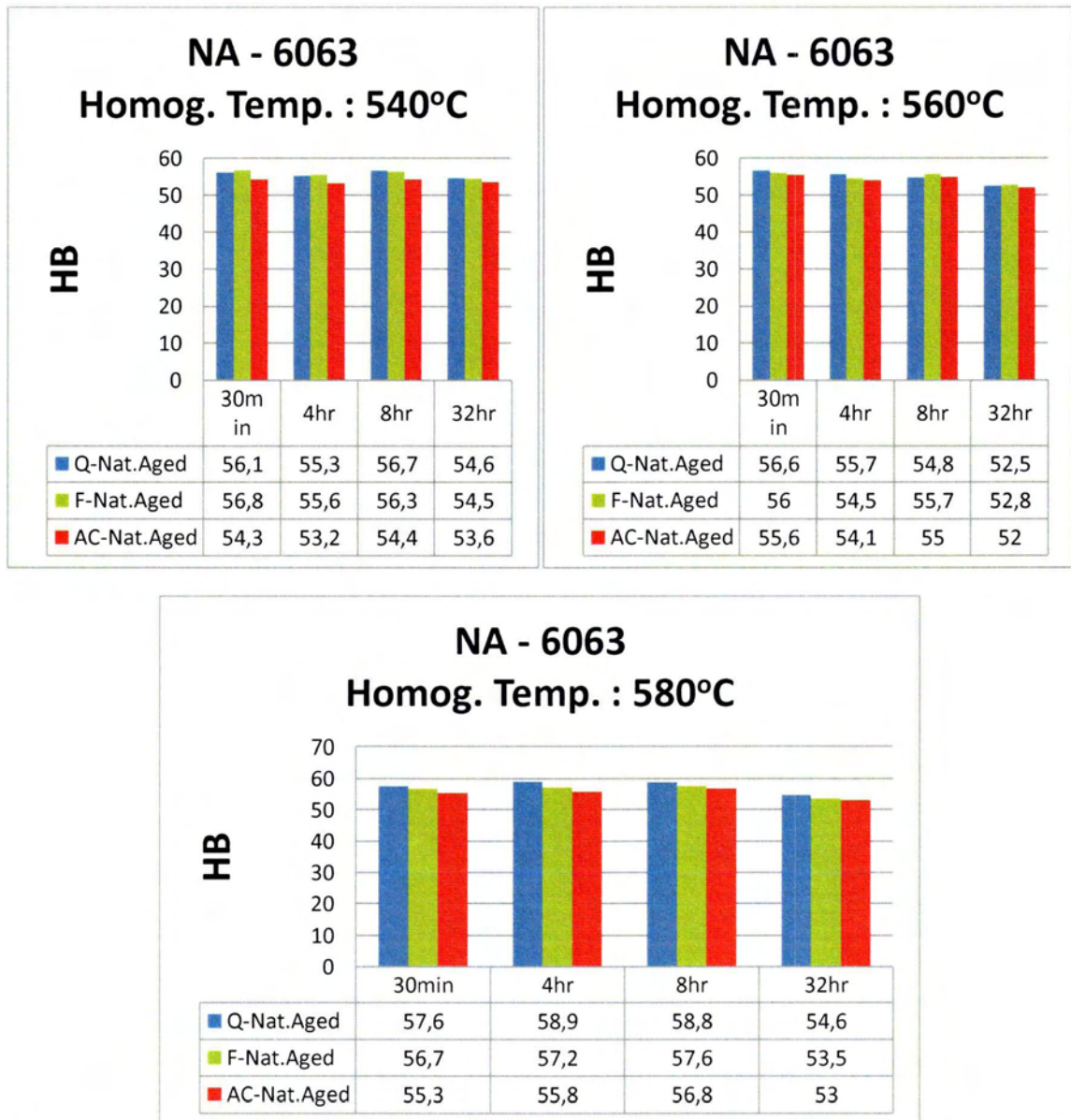


Fig.4.206082 Brinell hardness of the natural aged samples (NA) homogenized, a) at 540oC, b) at 560oC and c) at 580oC



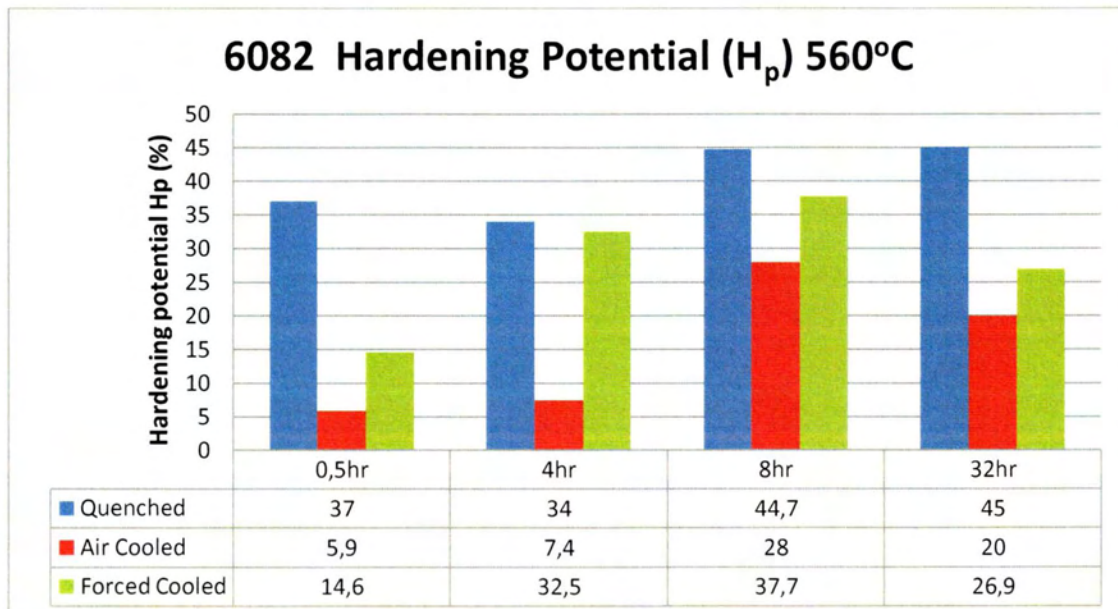
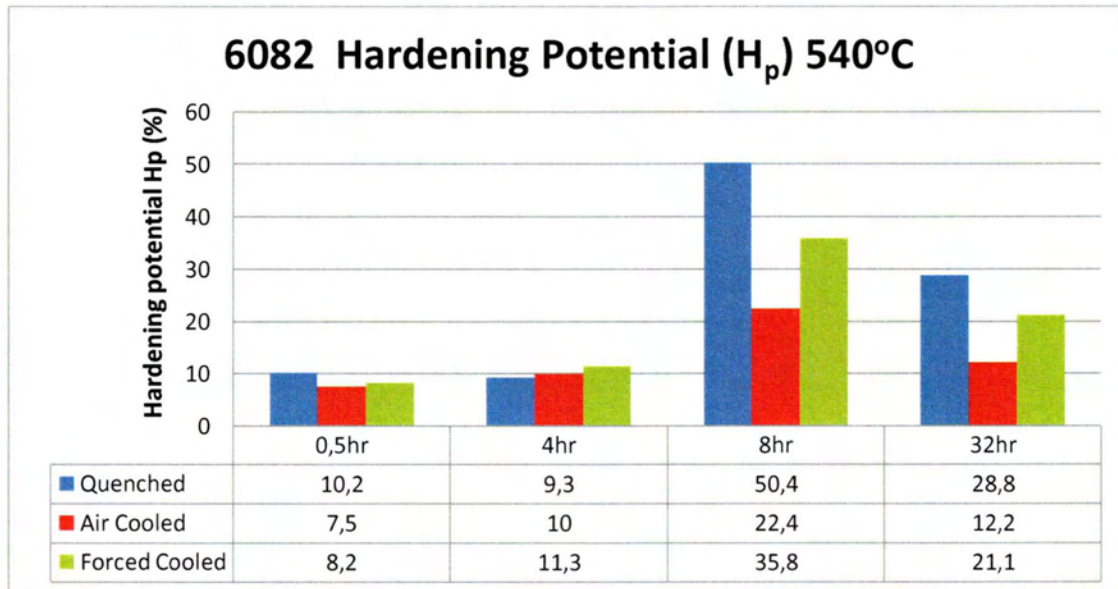
**Fig.4.21** 6082 Brinell hardness of the natural aged samples (NA) homogenized, a) at 540oC, b) at 560oC and c) at 580oC

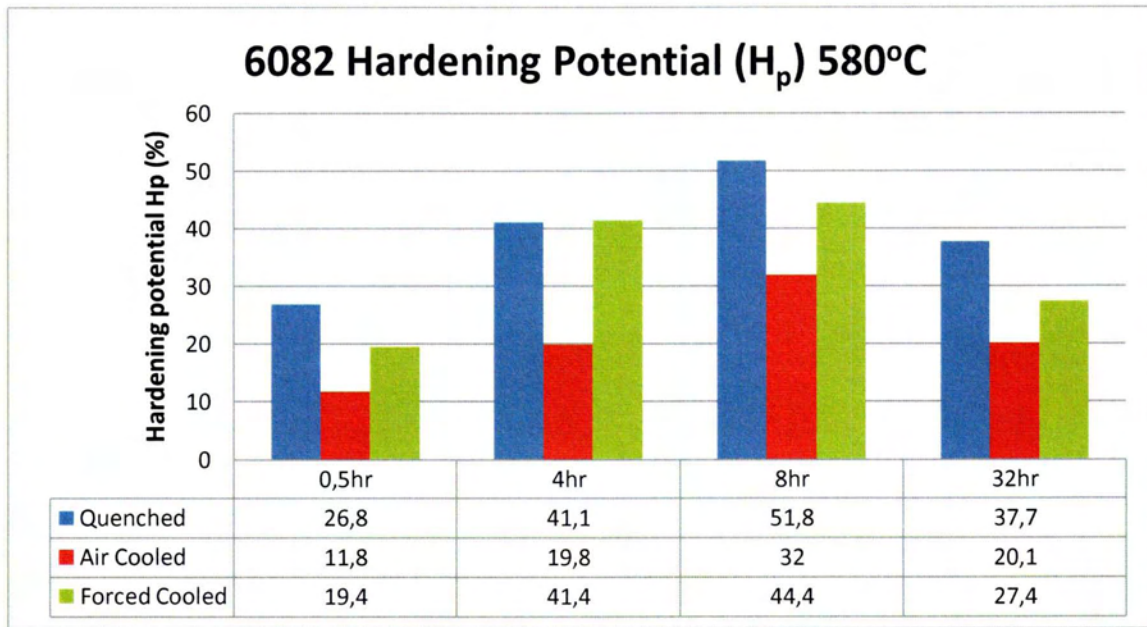
A very significant result of the hardness measurements is that the samples homogenized for 8hr at each temperature had the lower hardness but in contrast they had the larger age hardening potential. In short, they had the most significant percentage increase in hardness. (Figures 4.22-24) The hardening potential due to natural ageing can be defined as,

$$H_p = \frac{H_{NA} - H_{AH}}{H_{AH}} \times 100 \quad (4.2)$$

Considering these results, it seems that a significant factor controlling the selection of suitable homogenization temperature and time is the hardening potential  $H_p$ , in addition to the  $Mg_2Si$  dissolution and the  $\beta\text{-AlFeSi}$  to  $\alpha\text{-AlFeSi}$  transformation.

The relatively high supersaturation of atoms and vacancies retained by rapid quenching offers the maximum capacity for precipitation, namely age hardening potential. This fact is confirmed of the diagrams extracted from the natural aged samples **Fig. 4.16-18**, where the hardening of the water quenched specimens was much higher than on the other specimens cooled on different but lower rates. Taking a look on the lines of **Fig. 4.16-18** we can conclude that with decreasing cooling rate the hardness decreases. That is something we were waiting from the literature and applies for all the three alloys.





**Fig.4.22** 6082 alloy age hardening potential at 540, 560 and 580°C for every homogenization time.



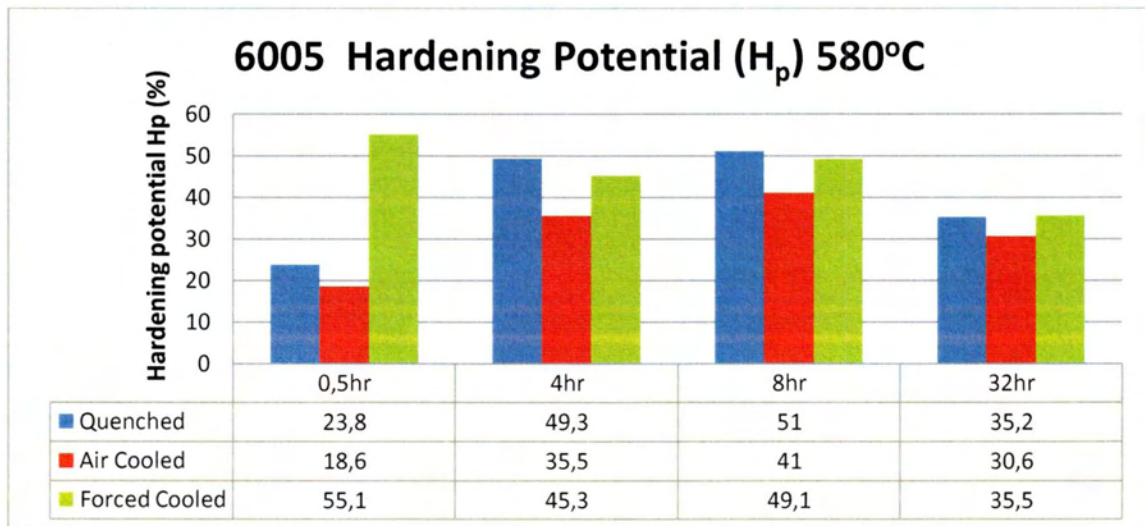
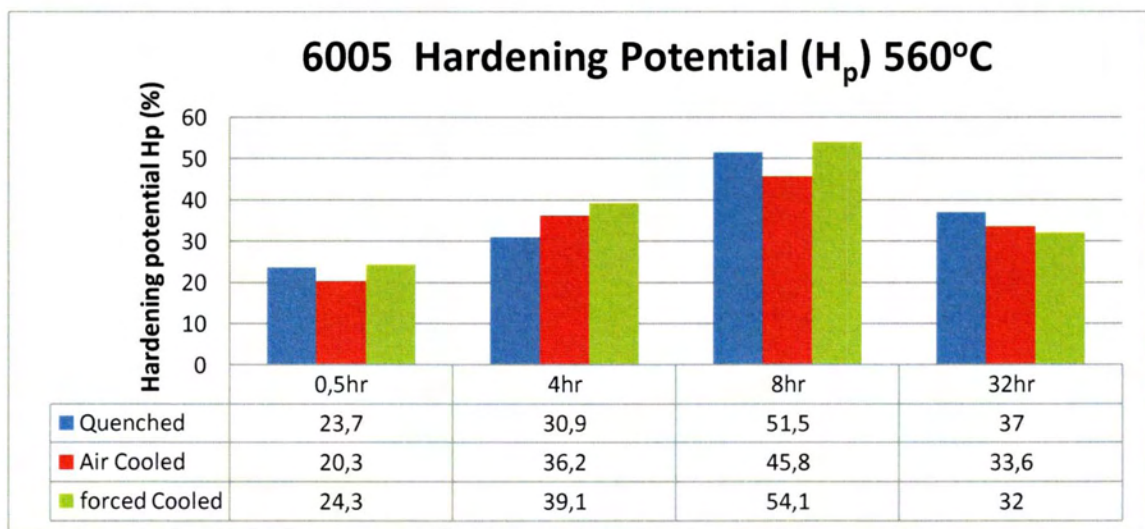
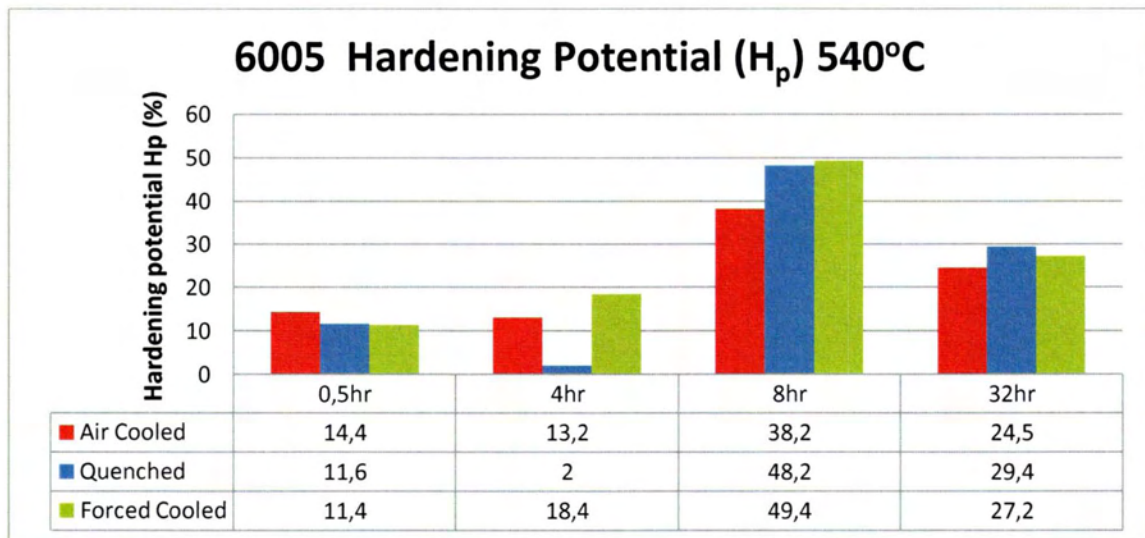


Fig.4.23 6082 alloy age hardening potential at 540, 560 and 580oC for every homogenization time.

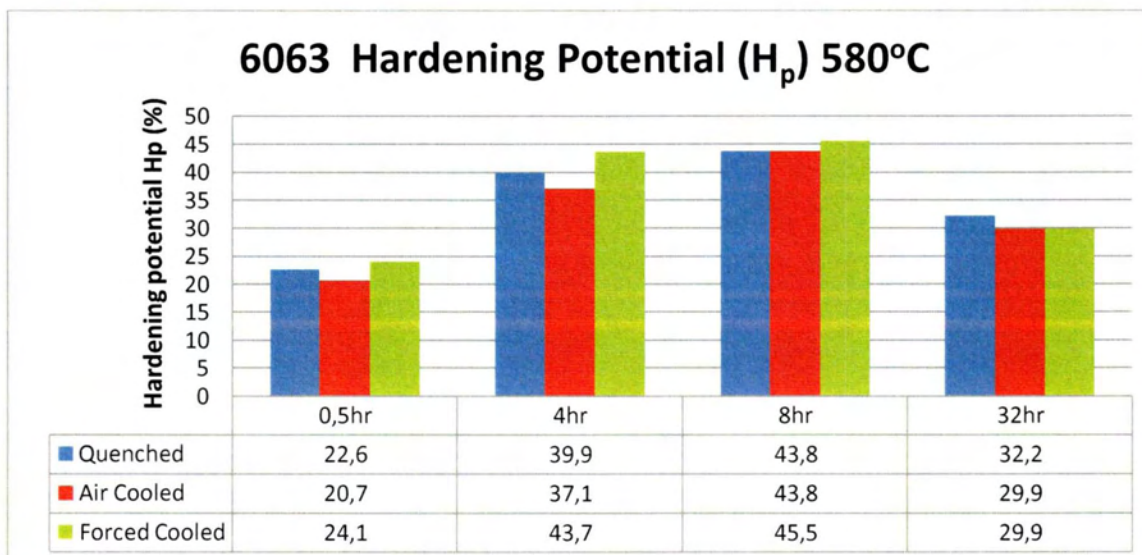
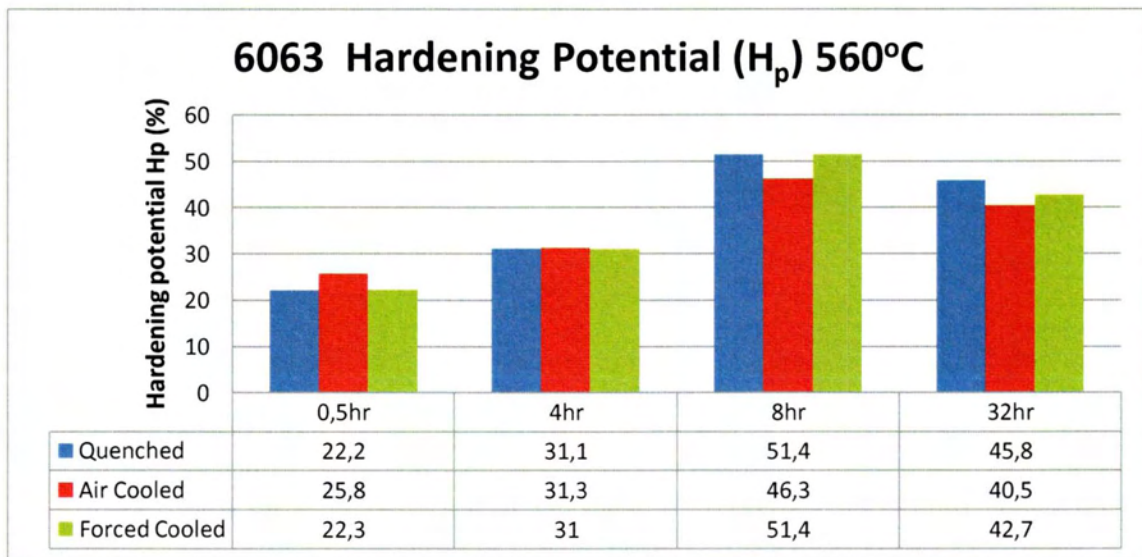
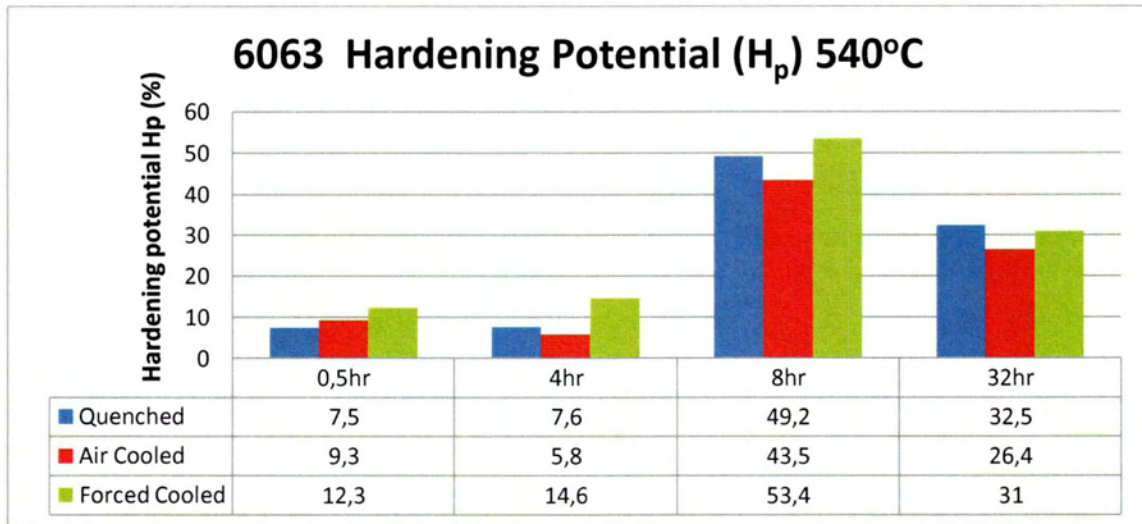


Fig.4.24 6082 alloy age hardening potential at 540, 560 and 580oC for every homogenization time.

# Chapter 5

## Conclusions

*In this chapter the main conclusions of the dissertation will be briefly presented.*

In the present dissertation the effect of the homogenization time and temperature and the cooling practice on the hardness and microstructure evolution, has been studied in three different aluminum alloys of the 6xxx series (6005, 6063, 6082). Metallographic observations, in the as-cast as well as in the as-homogenized condition of 6082 alloy, have been conducted. In addition quantitative metallography has been performed in order to measure the area fraction of the intermetallic phases of the alloy.

The main conclusions of this study are as follows:

**Effect of alloying elements:**

- The overall hardness values obtained from 6005 and 6063 alloys are lower than those obtained from 6082 and this is attributed to the lower Mg and Si compositions.
- The alloys with low Mg and Si levels, 6005 and 6063, gave almost identical Brinell hardness numbers for temperatures 560 and 580°C.

**Effect of homogenization temperature:**

- The microstructural changes are more prominent at 580°C. After a homogenization time of 8 hours the interdendritic platelets were replaced almost entirely of discrete round particles with a "necklace" configuration.
- For lower temperatures (e.g. 540°C), appreciable hardness changes take place on the transition of 4 to 8 hour homogenization, while at higher temperatures appreciable changes take place on the transition of 30 min to 4 hours homogenization.
- Higher homogenization temperatures lead to faster transformations. For a homogenization temperature of 540°C, homogenization time becomes the significant parameter.

**Effect of homogenization time:**

- Soaking at 540°C, 560°C and 580°C for 30 minutes seemed to have produced little change in the type and distribution of the intermetallic phases. There was no change in the morphology of the interdendritic particles and the transformation of the  $\beta$ -AlFeSi to  $\alpha$ -AlFe(Mn)Si was insignificant.
- Considerable morphological and microstructural changes were seen, starting at 4 hours of soaking. The  $\beta$  phase started to break up into small discrete particles.
- The hardness was influenced even for an 8hr soaking, although the Mg and Si composition gradients were zero. This is because diffusion of the Mg and Si elements does not only depend on the composition gradients, but on the chemical potential gradients of other elements such as Fe, Mn which were not zero.
- A slight increase in hardness is observed on the transition from 8 to 32 hours of soaking. It is attributed either to the dissolution of the quaternary eutectics or to the finer distribution of the Mg<sub>2</sub>Si particles.
- The samples homogenized for 8hr at each temperature showed the lowest hardness but in contrast they exhibited the highest age hardening potential.

### **Effect of cooling rate**

- The  $Mg_2Si$  distribution in the air-cooled specimens is more uniform than in the water-quenched specimens.
- The highest strength of the water cooled 6082 samples is attributed to solid solution strengthening.
- The  $Mg_2Si$  particles inside the dendrites increased with decreasing cooling rate providing higher Brinell hardness to the air cooled specimens than the forced air cooled ones of the 6082 alloy.
- The specimens which were cooled naturally in the air (AC) and those by forced cooling (FC) did not show any considerable difference in hardness.
- By decreasing cooling rate the hardness decreases in the naturally aged measurements.

## **Recommendation for further research**

Because the cooling rates used for this work were not close to those that are used in the industry, it would be an option for further research to repeat the same experiment using different cooling rates.

- Regarding the 6005 and 6063 alloys lower homogenization temperatures could be used, as we concluded in this work that the 560 and 580°C were relatively high and the results were normalized.
- More accurate work should be applied in more micrographs, in order to validate the quantitative results and to get statistically valid results.

## References

1. O. Reiso, "Extrusion of AlMgSi Alloys", MATERIALS FORUM, 28, (2004), 32-46
2. A. Jackson, T. Sheppard, "Aluminum Alloy Selection and Applications", Aluminum association Inc., 1, (1998), 1-20
3. Samaras, "Microstructure evaluation of heat treatments during extrusion of aluminum alloys", PhD, University of Thessaly, Volos, Greece, (2006)
4. Yücel Birol, "The effect of homogenization practice on the microstructure of AA6063 billets", J. Mat. Proc. Tech., 148, (2004), 250-258
5. Yucel Birol, "Homogenization of direct chill cast AlSi1MgMn billets", Int. J. Mater. Res. 105 (2014), 75-82
6. Tanihata, H et.al, "Effect of casting and homogenizing treatment conditions on the formation of Al-Fe-Si intermetallic compounds in 6063 Al-Mg-Si alloys", 4, (1989), 1205-1210
7. European Aluminum Association, "The automotive manual", (2002)
8. Hideji Suzuki et al., "Dislocations in solids", Yamada Conference IX, (1985)
9. J.P.Hirth, J.Lothe, "Theory of dislocations", 2<sup>nd</sup> Edition, Wiley Interscience Publications, NY, (1982)
10. J.D.Robson, P.B.Prangnell, "Dispersoid precipitation and process modelling in zirconium containing commercial aluminium alloys", Acta Materialia, 49, (2001), 599-613
11. J.W. Martin, "Precipitation Hardening", 2nd ed., Butterworth-Heinemann, Oxford, UK, (1998)
12. Kuijpers, N.C.W., "The dependence of the  $\beta$ -AlFeSi to  $\alpha$ -Al(FeMn)Si transformation kinetics in Al-Mg-Si alloys on the alloying elements", Thesis (2005)
13. S. Zajac, B. Hutchinson, A. Johansson and L.O. Gullman: *Microstructure control and extrudability of Al-Mg-Si alloys microalloyed with manganese*. Mat. Sci. Tech. 10 (1994), 323-333
14. Kuijpers, Niels C W, "A Model of the  $\beta$ -AlFeSi to  $\alpha$ -Al(FeMn)Si Transformation in Al-Mg-Si Alloys", Materials Transactions, 44, 7, (2003), 1448-1456
15. Saha P.K. "Aluminum Extrusion Technology", ASM International, Materials Park, Ohio, (2000)
16. A.r. Eivani, h. Ahmed, j. Zhou, "Evolution of Grain Boundary Phases during the Homogenization of AA7020 Aluminum Alloy", Metallurgical and materials transactions A, vol.40A, (2009)
17. Jimmy De Wilde. "Multicomponent, multiphase solidification: microstructure formation during the ternary eutectic reaction", Thesis, Katholieke Universiteit Leuven, (2005)
18. P. Castanya, et al., "Influence of quench rate and microstructure on bendability of AA6016 aluminium alloys", Materials Science and Engineering, A 559 (2013) 558-565

19. S. Zajac, B. Bengtsson, C. Jonsson, "Influence of cooling rate after homogenization and reheating to extrusion on extrudability and final properties of 6082 and 6063 alloys" Materials Science Forum, Trans Tech Publications, Switzerland, (2002)
20. Jorgen Van de Langkruis, "The effect of thermal treatments on the extrusion behavior of AlMgSi alloys", Thesis, (2000)
21. Kemal Deliji, Vanja Asanovi, Dragan Radonji, "The influence of the extrusion process and heat treatment on the properties of some AA6xxx extruded profiles", MTAEC9, 39(4)101, (2005)
22. Halfdan Kristoffer Småbråten, "Characterization of precipitates at maximum hardness and overaged conditions in Al-Mg-Si alloys", Thesis, Norwegian University of Science and Technology - Department of Materials Science and Engineering, (2011)
23. Yucel Birol, "Precipitation during homogenization cooling in AlMgSi alloys", Trans. Nonferrous Met. Soc. China 23(2013) 1875–1881
24. Yucel Birol, "Effect of cooling rate on precipitation during homogenization cooling in an excess silicon AlMgSi alloy", Materials Characterization, 73, (2012), 37-42
25. Grazyna Mrowka-Nowotnik, Jan Sieniawski, "Influence of heat treatment on the microstructure and mechanical properties of 6005 and 6082 aluminium alloys", Journal of Materials Processing Technology, 162-163, (2005), 367-372
26. Usta M. et al., "The effect of heat treatment on Mg<sub>2</sub>Si coarsening in aluminum 6105 alloy", Metallurgical and Materials Transactions A, 35A, (2004), 435
27. Samaras, S.N. Haidemenopoulos, G.N., "Modelling of microsegregation and homogenization of 6061 extrudable Al-alloy", Journal of Materials Processing Technology, 194, (2007), 63-73
28. Haidemenopoulos, G.N. Kamoutsi, H. Zervaki, A.D., "Simulation of the transformation of iron intermetallics during homogenization of 6xxx series extrudable aluminum alloys", Journal of Materials Processing Technology, 212, (2012), 2255-2260
29. P.I. Sarafoglou, G.N. Haidemenopoulos, "Computational thermodynamics investigation of the effects of alloying elements on intermetallic phase formation in the as cast microstructure of extrudable AlMgSiFeMn alloys", Elsevier Journal, (2013)
30. M. A. Abdel-Rahman et al., "Testing Natural Aging Effect on Properties of 6066 & 6063 Alloys using Vickers Hardness and Positron Annihilation Lifetime Techniques", Defect and Diffusion Forum, 303-304 (2010), 107-112
31. John Banhart, Cynthia Sin Ting Chang et al., "Natural ageing in Al-Mg-Si alloys – a process of unexpected complexity", Advanced Engineering Materials 12 (7), (2010) 559-571
32. S. Pogatscher et al., "Diffusion on Demand to Control Precipitation Aging: Application to Al-Mg-Si Alloys", PRL 112, (2014), 225701-1-5
33. M. A. van Huis, J. H. Chen, M. H. F. Sluiter, H. W. Zandbergen, "Phase stability and structural relations of nanometer-sized, matrix-embedded precipitate phases in Al-Mg-Si alloys in the late stages of evolution", Acta Mater., 54, (2006), 2945–2955
34. Matsuda K. et al., "Precipitation sequence of various kinds of metastable phases in Al alloys", Journal of Materials Science, 35, (2000), 179-189



35. Mariora C.D. et al, "Post- $\beta$ " phases and their influence on microstructure and hardness in 6xxx almgSi alloys", J.Mate.Sci., 41, (2006), 471-478
36. W.F. Miao and D.E. Laughlin., "Precipitation hardening in aluminum alloy 6022", Scripta Materialia, Vol. 40-7, (2001) 873-878,
37. Takeda M, Ohkubo F., "Stability of metastable phases and microstructures in the ageing process of AlMgSi ternary alloys", Journal of Materials science, 33, (1998), 2385-2390
38. Spiliopoulou Elisavet, "Microstructure characterization of aluminum 6061 during homogenization treatment", (2004)
39. ASTM Handbook Volume 2, " Properties and Selection Nonferrous", 1986, USA
40. ASTM Handbook Volume 4, " Heat Treating" , 1986, USA
41. ASTM Handbook Volume 8, " Mechanical Testing And Evalua" , 1986, USA
42. ASTM Handbook Volume 9, " Metallography and Microstructures" , 1986, USA
43. ASTM Handbook Volume 15, " Casting" , 1986, USA

## Appendix

### 1. Spheroidization mechanism of the $\beta$ -AlFeSi to $\alpha$ -Al(FeMn)Si transformation

In the previous paragraphs we used the term “extrudability”. This extrudability is qualitatively defined by the maximum production speed attainable for a given press capacity while still obtaining the desired mechanical properties, surface quality and geometric tolerances of the extrudate. As described earlier, the extrudability increases due to the  $\beta$  to  $\alpha$  transformation. The sharp tips of the  $\beta$  particles initiate micro-cracks during the deformation, and therefore start cracking the aluminium surface. The transformed  $\alpha$ -particles are more rounded and therefore cause less local cracking at the surface.

The proposed mechanism of the spheroidization of the GB particles is illustrated in Fig.2, based on the experimental observations from the FEG-SEM images (a typical one is shown in Fig.1) - (done by Ali Reza Eivani , “Modeling of Microstructural Evolution during Homogenization and Simulation of Transient State Recrystallization leading to Peripheral Coarse Grain Structure in Extruded Al-4.5Zn-1Mg Alloy”).

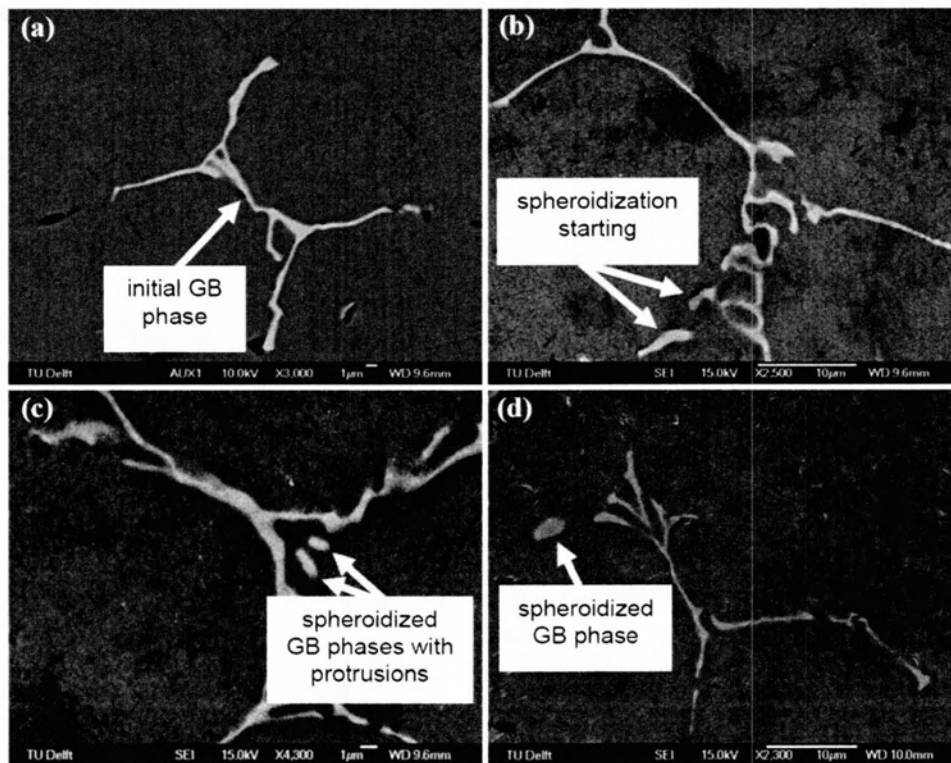
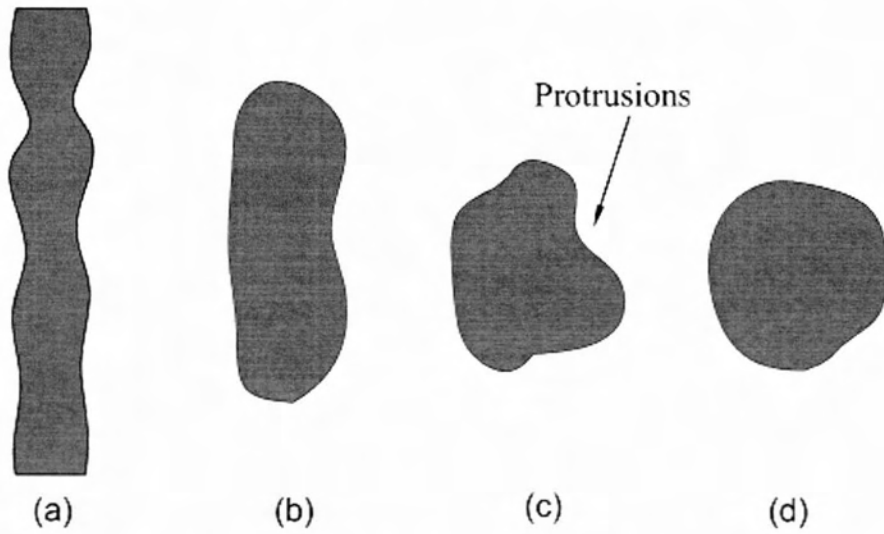


Fig.1 Typical shapes of grain boundary particles after homogenization of the alloy at 390°C, a) initial, b) 2, c) 8 and d) 24hr

Fig. 2(a) shows a grain boundary particle with initial protrusions on its surfaces. Afterwards, spheroidization occurs and the grain boundary particle takes an ellipse shape, Fig.

2(b). The spheroidization continues till the grain boundary particle takes a spherical shape with protrusions on its surface, Fig 2(c), and the process ends with removing the protrusions till the grain boundary particle resembles a sphere, Fig. 2(d). The driving force for spheroidization is the decrease in the surface energy of the GB particles with decreasing interfacial length between the GB particles and the aluminum matrix.



**Fig.2** Schematic view of the spheroidization mechanism

## 2. Specimen regularization tables

### 2.1 6082 aluminum alloy

Homogenization Temperature <b>540°C</b>		Quenching Treatment			Homogenization Temperature <b>560°C</b>		Quenching Treatment		
		Water Cooling (rapid) - WC/Q	Air Cooling - AC	Forced Cooling - FC			Water Cooling (rapid) - WC/Q	Air Cooling - AC	Forced Cooling - FC
Homogenization Time [=] hr	<b>0.5</b>	D4D <sub>0.5</sub> Q (19)	D4D <sub>0.5</sub> AC (20)	D4D <sub>0.5</sub> F (21)	Homogenization Time [=] hr	<b>0.5</b>	D6D <sub>0.5</sub> Q (22)	D6D <sub>0.5</sub> AC (23)	D6D <sub>0.5</sub> F (24)
	<b>4</b>	D4H <sub>4</sub> Q (82)	D4H <sub>4</sub> AC (83)	D4H <sub>4</sub> F (84)		<b>4</b>	D6H <sub>4</sub> Q (91)	D6H <sub>4</sub> AC (92)	D6H <sub>4</sub> F (93)
	<b>8</b>	D4H <sub>8</sub> Q (85)	D4H <sub>8</sub> AC (86)	D4H <sub>8</sub> F (87)		<b>8</b>	D6H <sub>8</sub> Q (94)	D6H <sub>8</sub> AC (95)	D6H <sub>8</sub> F (96)
	<b>32</b>	D4H <sub>32</sub> Q (88)	D4H <sub>32</sub> AC (89)	D4H <sub>32</sub> F (90)		<b>32</b>	D6H <sub>32</sub> Q (97)	D6H <sub>32</sub> AC (98)	D6H <sub>32</sub> F (99)

Homogenization Temperature <b>580°C</b>		Quenching Treatment		
		Water Cooling (rapid) - WC/Q	Air Cooling - AC	Forced Cooling - FC
Homogenization Time [=] hr	<b>0.5</b>	D8D <sub>0.5</sub> Q (25)	D8D <sub>0.5</sub> AC (26)	D8D <sub>0.5</sub> F (27)
	<b>4</b>	D8H <sub>4</sub> Q (100)	D8H <sub>4</sub> AC (101)	D8H <sub>4</sub> F (102)
	<b>8</b>	D8H <sub>8</sub> Q (103)	D8H <sub>8</sub> AC (104)	D8H <sub>8</sub> F (105)
	<b>32</b>	D8H <sub>32</sub> Q (106)	D8H <sub>32</sub> AC (107)	D8H <sub>32</sub> F (108)

## 2.2 6005 aluminum alloy

Homogenization Temperature <b>540°C</b>		Quenching Treatment			Homogenization Temperature <b>560°C</b>		Quenching Treatment		
		Water Cooling (rapid) - WC/Q	Air Cooling - AC	Forced Cooling - FC			Water Cooling (rapid) - WC/Q	Air Cooling - AC	Forced Cooling - FC
Homogenization Time [=] hr	0.5	C4D <sub>0.5</sub> Q (1)	C4D <sub>0.5</sub> AC (2)	C4D <sub>0.5</sub> F (3)	Homogenization Time [=] hr	0.5	C6D <sub>0.5</sub> Q (4)	C6D <sub>0.5</sub> AC (5)	C6D <sub>0.5</sub> F (6)
	4	C4H <sub>4</sub> Q (28)	C4H <sub>4</sub> AC (29)	C4H <sub>4</sub> F (30)		4	C6H <sub>4</sub> Q (37)	C6H <sub>4</sub> AC (38)	C6H <sub>4</sub> F (39)
	8	C4H <sub>8</sub> Q (31)	C4H <sub>8</sub> AC (32)	C4H <sub>8</sub> F (33)		8	C6H <sub>8</sub> Q (40)	C6H <sub>8</sub> AC (41)	C6H <sub>8</sub> F (42)
	32	C4H <sub>32</sub> Q (34)	C4H <sub>32</sub> AC (35)	C4H <sub>32</sub> F (36)		32	C6H <sub>32</sub> Q (43)	C6H <sub>32</sub> AC (44)	C6H <sub>32</sub> F (45)

Homogenization Temperature <b>580°C</b>		Quenching Treatment		
		Water Cooling (rapid) - WC/Q	Air Cooling - AC	Forced Cooling - FC
Homogenization Time [=] hr	0.5	C8D <sub>30</sub> Q (7)	C8D <sub>30</sub> AC (8)	C8D <sub>30</sub> F (9)
	4	C8H <sub>4</sub> Q (46)	C8H <sub>4</sub> AC (47)	C8H <sub>4</sub> F (48)
	8	C8H <sub>8</sub> Q (49)	C8H <sub>8</sub> AC (50)	C8H <sub>8</sub> F (51)
	32	C8H <sub>32</sub> Q (52)	C8H <sub>32</sub> AC (53)	C8H <sub>32</sub> F (54)

### 2.3 6063 aluminum alloy

Homogenization Temperature <b>540°C</b>		Quenching Treatment			Homogenization Temperature <b>560°C</b>		Quenching Treatment		
		Water Cooling (rapid) - WC/Q	Air Cooling - AC	Forced Cooling - FC			Water Cooling (rapid) - WC/Q	Air Cooling - AC	Forced Cooling - FC
Homogenization Time [=] hr	0.5	B4D <sub>0.5</sub> Q (10)	B4D <sub>0.5</sub> AC (11)	B4D <sub>0.5</sub> F (12)	Homogenization Time [=] hr	0.5	B6D <sub>0.5</sub> Q (13)	B6D <sub>0.5</sub> AC (14)	B6D <sub>0.5</sub> F (15)
	4	B4H <sub>4</sub> Q (55)	B4H <sub>4</sub> AC (56)	B4H <sub>4</sub> F (57)		4	B6H <sub>4</sub> Q (54)	B6H <sub>4</sub> AC (65)	B6H <sub>4</sub> F (66)
	8	B4H <sub>8</sub> Q (58)	B4H <sub>8</sub> AC (59)	B4H <sub>8</sub> F (60)		8	B6H <sub>8</sub> Q (57)	B6H <sub>8</sub> AC (68)	B6H <sub>8</sub> F (69)
	32	B4H <sub>32</sub> Q (61)	B4H <sub>32</sub> AC (62)	B4H <sub>32</sub> F (63)		32	B6H <sub>32</sub> Q (70)	B6H <sub>32</sub> AC (71)	B6H <sub>32</sub> F (72)

Homogenization Temperature <b>580°C</b>		Quenching Treatment		
		Water Cooling (rapid) - WC/Q	Air Cooling - AC	Forced Cooling - FC
Homogenization Time [=] hr	0.5	RRD <sub>0.5</sub> Q (16)	RRD <sub>0.5</sub> AC (17)	RRD <sub>0.5</sub> F (18)
	4	B8H <sub>4</sub> Q (73)	B8H <sub>4</sub> AC (74)	B8H <sub>4</sub> F (75)
	8	B8H <sub>8</sub> Q (76)	B8H <sub>8</sub> AC (77)	B8H <sub>8</sub> F (78)
	32	B8H <sub>32</sub> Q (79)	B8H <sub>32</sub> AC (80)	B8H <sub>32</sub> F (81)

ΠΑΝΕΠΙΣΤΗΜΙΟ ΘΕΣΣΑΛΙΑΣ  
ΒΙΒΛΙΟΘΗΚΗ



004000121295

